AoI-minimal Clustering, Transmission and Trajectory Co-design for UAV-assisted WPCNs

Xiaoying Liu, *Senior Member, IEEE*, Huihui Liu, Kechen Zheng, *Senior Member, IEEE*, Jia Liu, *Senior Member, IEEE*, Tarik Taleb, *Senior Member, IEEE*, Norio Shiratori, *Life Fellow, IEEE*

***Abstract*—This paper investigates the long-term average age of information (AoI)-minimal problem in an unmanned aerial vehicle (UAV)-assisted wireless-powered communication network (WPCN), which consists of a static hybrid access point (HAP), a mobile UAV, and many static sensor nodes (SNs) randomly distributed on multiple islands. The UAV first is fully charged by the HAP, and then flies to each island to charge SNs and receive data from them. Before running out the energy in battery, the UAV flies back to the HAP to offload the received data and be fully charged again. Due to the finite battery capacity of the UAV, it is impossible for the UAV to traverse all the islands to collect all the data from SNs for once flight. We are thus inspired to divide islands into multiple clusters so that the UAV could traverse all the islands in each cluster. The key factors affecting the long-term average AoI contain the hovering duration, the flying duration, and the amount of data from each island reflected by the number of SNs on each island. Therefore, we formulate the long-term average AoI-minimal problem by jointly optimizing the transmit power of SNs, clustering of islands, and UAV's flight trajectory, subject to the battery capacity of the UAV. Since the optimization problem is NP-hard, there are no standard methods to solve it optimally in general. To tackle this problem, we decouple it into two subproblems: the power allocation subproblem for SNs, and the joint clustering of islands and UAV's flight trajectory design subproblem, which is much more perplexed and complicated owing to the tight coupling between them. To solve the first subproblem, we propose a hybrid TDMA and NOMA (HTN) protocol that takes advantage of the two protocols. To solve the second subproblem, we propose a clustering-based dynamic adjustment of the shortest path (C-DASP) algorithm, which is composed of three sub-algorithms, i.e, a proposed merging-aided K-means clustering (MaKMC) algorithm, the particle swarm optimization (PSO) algorithm employed to find the shortest path in each cluster, and a proposed dynamic adjustment (DA) algorithm taking into account the number of SNs on each island. Simulations verify the effectiveness and superiority of the proposed HTN protocol and C-DASP algorithm.**

This work was supported in part by the National Natural Science Foundation of China under Grant 62372412 and Grant 62372413; in part by the Fundamental Research Funds for the Provincial Universities of Zhejiang under Grant RF-A2022005; in part by JSPS KAKENHI Grant Number JP23K16877; and in part by the Project of Cyber Security Establishment with Inter-University Cooperation.(*Corresponding author: Kechen Zheng.*)

X. Liu, H. Liu, and K. Zheng are with the School of Computer Science and Technology, Zhejiang University of Technology, China. E-mail: {xiaoyingliu, 2112112126, kechenzheng}@zjut.edu.cn.

J. Liu is with the Center for Strategic Cyber Resilience Research and Development, National Institute of Informatics, Tokyo 101-8430, Japan. Email: jliu@nii.ac.jp.

T. Taleb is with the Faculty of Electrical Engineering and Information Technology, Ruhr University Bochum, Bochum 44801, Germany. E-mail: tarik.taleb@rub.de.

N. Shiratori is with the Research and Development Initiative, Chuo University, Tokyo 112-8551, Japan. E-mail: norio.shiratori.e8@tohoku.ac.jp.

***Index Terms*—Unmanned aerial vehicle, wireless powered communication networks, age of information, trajectory design.**

I. Introduction

A. Background

By unifying the technologies of wireless power transfer (WPT) and wireless information transfer (WIT), wireless powered communication network (WPCN) has emerged as a promising technique to provide ubiquitous wireless energy and data transmission for a massive number of low-power wireless nodes (WNs) in the upcoming Internet of Things (IoT) era [1]. A typical WPCN consists of a hybrid access point (HAP) and multiple WNs with energy harvesting capability. The HAP first broadcasts the radio frequency (RF) signal to charge WNs via WPT in the downlink, and then WNs utilize the harvested energy to send their data back to the HAP via WIT in the uplink [2]. In general, once the HAP is deployed, it is fixed and cannot be moved. As a result, there are several issues that the WPCN with the fixed HAP has to be confronted with. First, due to the severe RF signal propagation loss over distance, the energy transfer efficiency degrades seriously when the distance between the HAP and WNs becomes large. Second, when multiple WNs are distributed at different locations in a WPCN, the WNs far away from the HAP harvest less energy, but conversely need to consume more energy to achieve the same quality of service (QoS) as the WNs located near the HAP, thus leading to a critical near-far fairness issue [3].

To deal with the above issues, the unmanned aerial vehicle (UAV) has been incorporated as a mobile access point to transmit the RF signal and collect the data in WPCNs, due to its advantages in flexible deployment and controllable mobility [4], [5]. To be specific, as the UAV flies near some WNs, the qualities of links between the UAV and these WNs become better, and accordingly it is more efficient for the UAV to charge these WNs and collect data from them. Therefore, the UAV-assisted WPCN architecture with UAVs playing the role of mobile access points is supported as an extraordinary approach to address the two issues [6]. The available works on the UAV-assisted WPCNs mainly focused on the energy-related optimization [7], [8] aiming to extend the network lifetime and the throughput-related optimization [9], [10] by separately or jointly optimizing the flight trajectory, resources allocation, etc.

Thanks to the aforementioned UAV's advantages, the UAV has been applied in the emerging time-sensitive applications, such as environmental monitoring [11] and remote control [12]. In such applications, the generated data needs to be

TABLE I: Differences between this paper and the related works

Reference	Minimization objective	Number (UAV)	Clustering	Energy harvesting (WN)	Battery recharging (UAV)	Energy constraint (UAV)
[16]	Weighted average AoI	one	×	×	×	√
[17]	Average peak AoI	one	×	×	×	√
[18]	Total AoI	one	√	×	×	×
[19], [20]	Average AoI	one	×	√	×	×
[21], [22]	Expected AoI	multiple	×	√	×	√
[23]	Average AoI cost	one	×	×	√	√
[24]	Joint weighted average AoI and WDs' transmission power	multiple	√	×	√	√
This paper	Long-term average AoI	one	√	√	√	√

[1] √ denotes the existence of the feature; × denotes the absence of the feature.

delivered to the destination as soon as possible for further data analyzing and decision making, since outdated information can result in incorrect control and even disasters [13]. Therefore, it is essential to maintain the freshness of information received at the destination. To quantitatively characterize the freshness of information, a new performance metric, i.e., age of information (AoI) defined as the time elapsed since the generation of the most recently received data observed at the destination, has been proposed in [14]. Different from the traditional performance metrics such as throughput and delay, AoI has powerful capability on capturing the timeliness of information [15]. As such, AoI-oriented data collection has recently attracted increasing attention in UAV-assisted wireless networks.

B. Related works

Due to the finite battery capacity of the UAV, the critical issues in AoI-oriented UAV-assisted wireless networks are how to reasonably schedule the UAV and adjust the trajectory to save the total time of task achievement so as to minimize the AoI of the received data. Consequently, many works have been done to tackle the issues [16]–[18]. Yi *et al.* [16] used a deep Q-network (DQN) algorithm to find the optimal flight trajectory of the UAV and transmission scheduling of WNs that minimizes the sum AoI while considering the energy consumption of the UAV. Elmagid *et al.* [17] jointly optimized UAV's flight trajectory, energy allocations and service time for both WNs and UAV to minimize the overall peak AoI of the system. It should be noticed that the UAV in [16], [17] was dispatched to visit every WN, and the energy consumption of the UAV increases due to the increased flight trajectory. To reduce the energy consumption of the UAV, Zhu *et al.* [18] investigated a cluster-based IoT network, where all WNs are divided into multiple clusters and send data to their corresponding cluster heads (CHs). Thus the UAV only needs to interact with the CHs to receive the aggregated data, and accordingly the UAV's hovering points and trajectory are jointly optimized to minimize the total AoI.

However, the UAV in [16]–[18] just acted as the mobile data collector without the energy transmitter, causing that the energy supply of WNs has not been captured. Therefore, a few recent works have been carried out to study the AoI minimization problem in UAV-assisted WPCNs, where the UAV acts as not only the data collector but also the energy transmitter [19]–[22]. To be specific, considering a scenario where the UAV flies to every WN to transfer energy and receive data, Hu *et al.* [19] minimized the average AoI by jointly optimizing the UAV's flight trajectory and the time of energy harvesting for each WN. They decomposed the optimization problem into a hovering time allocation problem and a UAV's trajectory design problem, and solved them by the dynamic programming approach. For the similar optimization problem, Liu *et al.* [20] employed the deep reinforcement learning (DRL) approach to find a near-optimal solution. We notice that works [19], [20] did not take the energy constraint of the UAV into account, which is an essential factor in practice. Different from the above works, Oubbati *et. al* [21] deployed two UAVs in a WPCN, where one behaves as the energy transmitter to charge WNs and the other behaves as the data collector to collect the data from WNs, and aimed to minimize the expected AoI of all WNs by proposing a multi-agent DRL based UAVs' trajectories strategy. In [22], the authors extended the work in [21] to the scenario where UAVs are divided into two teams to behave as energy transmitters and data collectors, respectively. Differences between this paper and the related works are summarized in TABLE I.

C. Motivations and contributions

Nevertheless, the aforementioned works [16]–[22] focused on only one flight of UAV for data collection, i.e, the UAV flies from a station to visit a subset of WNs and then flies back to the station for data analysis. The UAV with battery recharging, enabling the UAV to perform multiple flights, has seldom been investigated in the literature. As far as we know, only works [23], [24] considered the battery recharging of the UAV. Nonetheless, the energy supply of WNs, i.e, the UAV acting as the energy transmitter, was not considered in the design of the UAV's trajectory, and the objectives of [23], [24] were not the average AoI minimization. As a result, little attention has been devoted to the AoI-minimal design in UAV-assisted WPCNs with the battery recharging of the UAV.

To fill this gap, we investigate the long-term average AoI minimization problem in a UAV-assisted WPCN where N wireless-powered sensor nodes (SNs) are randomly distributed on M islands to sense the environment and generate data, a static HAP is responsible for charging UAV and receiving data from UAV, and a battery-limited UAV acts as a mobile relay between SNs and the HAP. There are many application scenarios consisting of HAP/access point (AP), SNs and UAV, such as the building structural health monitoring [10] and the environmental monitoring [11]. To be specific, the UAV first is fully charged by the HAP, and then flies to a set of islands to charge SNs and receive data from them. Before running

out the energy in battery, the UAV flies back to the HAP to offload the received data and be fully charged again. In term of these, there are three challenges as follows. First, due to the finite battery capacity of the UAV, it is impossible for the UAV to traverse all the islands to collect all the data from SNs for once flight. Even if multiple UAVs are used for data collection at a high cost, it is difficult to ensure that all data is collected by once flight for every UAV. Thus, *the first challenge is how to divide the islands into multiple clusters to ensure that the fully-charged UAV could traverse all the islands in one cluster*. Second, since the UAV needs to hover over islands to transmit the RF signal to SNs and receive data from SNs, the hovering duration over one island is comprised of the energy transfer duration and the data transmission duration. Concerning the data transmission from multiple SNs on one island to the UAV, it is well known that nonorthogonal multiple access (NOMA) protocol has the potential to achieve lower transmission duration compared with time-division multiple access (TDMA) protocol, but may have higher energy requirements for some SNs [25]. Consequently, *the second challenge is how to design the transmission protocol of SNs on each island by taking advantage of the two protocols, to minimize the hovering duration and thereby minimize the long-term average AoI*. Third, another key factor affecting the long-term average AoI is the flight trajectory of the UAV. It is intuitively believed that when other factors are given and fixed, once the UAV flies according to the shortest path, the minimal average AoI could be achieved owing to the minimal flying duration. However, in our WPCN, the amount of data from each island, which is reflected by the number of SNs on each island, has a great effect on the long-term average AoI. Since the data from one island is received together, the long-term average AoI for the UAV traversing the islands with more SNs early would be larger than that for the UAV traversing the islands with more SNs later. Therefore, *the third challenge is how to design the flight trajectory of the UAV to minimize the long-term average AoI by taking both the flying duration and the number of SNs on each island into account*. Regarding the above challenges, we summary main contributions as follows.

- To our best knowledge, this is the first attempt to study the long-term average AoI-minimal problem in a UAV-assisted WPCN where the battery recharging of the UAV is taken into account, through jointly optimizing the transmit power of SNs, the clustering of islands, and the flight trajectory of the UAV.
- To address the NP-hard optimization problem, we decompose it into two subproblems: the power allocation subproblem for SNs, and the joint clustering of islands and UAV's flight trajectory design subproblem. To solve the first subproblem, we propose a hybrid TDMA and NOMA (HTN) protocol that takes advantage of the two protocols. Every time the UAV hovers over an island, the HTN protocol decides whether TDMA or NOMA should be adopted and the transmit power of SNs based on the residual energy of SNs. *This solution could tackle the second challenge*. To solve the second subproblem, we propose a clustering-based dynamic adjustment of the shortest path (C-DASP) algorithm, which is composed of three sub-algorithms, i.e, a proposed merging-aided K-means clustering (MaKMC) algorithm, the particle swarm optimization (PSO) algorithm for finding the shortest path in one cluster, and a proposed dynamic adjustment (DA) algorithm taking into account the number of SNs on each island. *This solution could tackle the first and third challenges*.
- Simulation results show that the proposed HTN protocol outperforms both the TDMA protocol and NOMA protocol in terms of the long-term average AoI, and meanwhile verify the superiority of the proposed C-DASP algorithm. Moreover, simulations demonstrate there is a tradeoff between the number of clusters and the total flying and hovering duration in one cluster resulted from the battery capacity of the UAV.

The rest of this paper is organized as follows. In Section II, we introduce the system model. In Section III, we formulate the AoI-minimal problem. In Section IV, we provide the solutions to the formulated problem. Then simulation results and discussions are presented in Section V. Finally, a conclusion is drawn in Section VI.

II. System Model

We introduce the UAV-assisted WPCN from four aspects: network model, energy transfer model, proposed HTN protocol, and AoI model. Wherein, the network model is first employed to study the average AoI-minimal problem, and the HTN protocol is proposed by this paper.

A. Network Model

We consider a novel scenario of the UAV-assisted WPCN. The UAV-assisted WPCN consists of a static HAP, N static SNs, and a mobile UAV, as shown in Fig. 1. The HAP, with location $(x_h, y_h, 0)$, is responsible for charging the UAV and receiving data from the UAV. N SNs are distributed on M non-overlapping islands in the area of WPCN. N_m represents the positive number of the SNs on island m, and satisfies

$$\sum_{m=1}^{M} N_m = N. \tag{1}$$

Let $S_{i,m}$ denote the ith ($i \in \{1, 2, \ldots, N_m\}$) SN on island m ($m \in \{1, 2, \ldots, M\}$), and $s_{i,m} = (x_{i,m}, y_{i,m}, 0)$ denote the location of $S_{i,m}$. Without loss of generality, the SNs on one island are sorted in a descending order of the gain of the channel between the SN and the UAV. Taking island m as an example, the gain of the channel between $S_{1,m}$ and the UAV is the highest, and the gain of the channel between $S_{N_m,m}$ and the UAV is the lowest. The SNs, equipped with energy harvesting components, first harvest energy from the RF signal of the UAV when the UAV flies to the hovering point of this island. Then the SNs sense the surroundings, generate data, and transmit the generated data to the UAV by consuming the harvested energy. Here we consider that the data generation is completed instantaneously. The process of data transmission from the SNs to the UAV will be specified in Section II-C.

Equipped with a battery of finite capacity $C_{\max}$, the fully-charged UAV flies to hovering points at a fixed height h

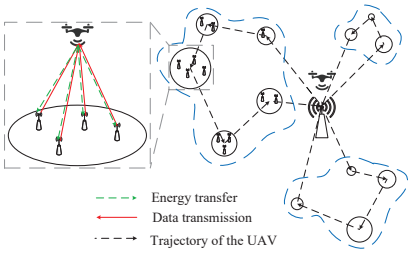

Fig. 1: The UAV-assisted WPCN.

by consuming the energy in the battery. There is only one hovering point on each island, denoted by U_m with location (x_m, y_m, h). When the UAV flies to hovering point U_m, it first transmits the RF signal to charge the SNs on island m during the energy transfer stage, and then receives data from SNs during the data transmission stage. After traversing the islands according to the predetermined flight trajectory, the UAV returns to the HAP to offload the received data, and is fully charged by the HAP for the next flight. The flight trajectory of the UAV will be introduced in Section IV-C.

Due to the finite battery capacity, the UAV could hardly traverse every island to receive data from all the SNs before being charged by the HAP. Thus we are motivated to divide M islands into K clusters as

$$\sum_{k=1}^{K} M_k = M, \tag{2}$$

where $M_k > 0$ denotes the number of islands in cluster k. It is worth noting that different from existing works [13], [18], [26], where SNs are clustered, a cluster head (CH) or data collection point (CP) is selected from each cluster, and the UAV visits each CH to collect the aggregated data or visits each CP to collect the data from SNs sequentially, we divide the islands, where several SNs are randomly distributed, into clusters due to the consideration of UAV's battery recharging. After the UAV is fully charged, it has enough energy to fly to every island in a cluster, charge SNs, receive data from SNs, and fly back to the HAP. Due to the advantages of simplicity, efficiency and stable performance of the K-means clustering (KMC) algorithm [27], we propose a merging-aided K-means clustering (MaKMC) algorithm to divide islands, and the clustering process will be introduced in Section IV-C. As depicted in Fig. 1, the fully-charged UAV, hovering over the HAP, selects cluster k according to the indexes given by the proposed MaKMC algorithm. Then the UAV traverses every island in cluster k to complete the tasks of energy transfer to SNs and data reception from SNs according to the predetermined flight trajectory, i.e., HAP $\rightarrow V_{1_k} \rightarrow \ldots \rightarrow V_{(M_k)_k} \rightarrow$ HAP, where V_{i_k} represents the i_kth traversed hovering point in the UAV's flight trajectory of cluster k, and $\{V_{1_k}, V_{2_k}, \ldots, V_{(M_k)_k}\}$ is an element of the set of the permutations of $\{U_1, U_2, \ldots, U_M\}$.

For the UAV above the hovering point U_m, let t_m^e denote the duration of the energy transfer stage, t_m^t denote the duration of the data transmission stage, and t_m^{hov} denote the total hovering duration of the UAV on island m, i.e., $t_m^{hov} = t_m^e + t_m^t$. After the UAV completes the data reception tasks from every SN in cluster k and flies back to the HAP, the UAV offloads the received data to the HAP with duration t_k^d, and is charged by the HAP with duration t_k^h. To facilitate the time analysis, we consider $t_k^d = t_d$ and $t_k^h = t_h$ for every cluster.

As pointed out in [28], channel qualities are mainly determined by the large-scale fading, so we consider that the channels in the UAV-assisted WPCN are dominated by the large-scale fading. The distance between U_m and $S_{i,m}$, denoted by $d_{i,m}$, is formulated as

$$d_{i,m} = \sqrt{(x_m - x_{i,m})^2 + (y_m - y_{i,m})^2 + h^2}. \tag{3}$$

Let $|g|^2$ denote the gain of the channel between the HAP and the UAV as $|g|^2 = \frac{\kappa}{h^\alpha}$, where κ denotes the reference signal gain at the distance of 1 meter, and $\alpha \in [2, 4]$ denotes the path-loss factor [19]. Let $|g_{i,m}|^2$ denote the gain of the channel between $S_{i,m}$ and U_m as $|g_{i,m}|^2 = \frac{\kappa}{d_{i,m}^\alpha}$.

B. Energy Transfer Model

During the energy transfer stage with duration t_m^e on island m, the UAV charges SNs on island m with power p_m^e, and the amount of the energy harvested by $S_{i,m}$, denoted by $E_{i,m}^h$, is

$$E_{i,m}^h = \eta p_m^e |g_{i,m}|^2 t_m^e, \tag{4}$$

where $\eta \in (0, 1)$ is the energy conversion efficiency [30]. Each SN stores the harvested energy in the battery with capacity E_{max}. When the UAV flies to island m for the ζth traversal, the energy of $S_{i,m}$ is updated as

$$E_{i,m}(\zeta) = E_{i,m}(\zeta - 1) + E_{i,m}^h - E_{i,m}^t(\zeta - 1), \tag{5}$$

where $E_{i,m}^t(\zeta - 1)$ denotes the energy consumed by $S_{i,m}$ for data transmission during UAV's $(\zeta - 1)$th traversal to island m.

Without loss of generality, the energy consumption of the UAV for traversing the islands in cluster k includes three parts: the energy consumption of flying E_k^f, the energy consumption of hovering E_k^{hov}, and the energy consumption of charging SNs E_k^{ch}. Based on the energy constraint, the energy consumption of traversing the islands in cluster k is no larger than the battery capacity of the UAV as

$$E_k^f + E_k^{hov} + E_k^{ch} \leqslant C_{\max}. \tag{6}$$

In the following, we analyze E_k^f at first. With respect to the propulsion power consumption model in [29], the power consumption of UAV flying at speed V, denoted by $P(V)$, is

$$P(V) = P_0\Big(1 + \frac{3V^2}{U_{tip}^2}\Big) + P_i\Big(\sqrt{1 + \frac{V^4}{4v_0^4}} - \frac{V^2}{2v_0^2}\Big)^{1/2} + \frac{d_0 \rho s A V^3}{2}, \tag{7}$$

where P_0 and P_i are two constants based on the physical properties of UAV and the flight environment, such as weight, rotor radius, and air density. U_{tip} denotes the tip speed of the rotor blade. v_0 is known as the mean rotor induced velocity when hovering. d_0 and s denote the fuselage drag ratio and rotor solidity, respectively. ρ and A denote the air density and rotor disc area, respectively. Then the energy consumption of flying E_k^f is given by

$$E_k^f = \frac{L_k}{V} P(V), \tag{8}$$

where L_k represents the distance of the flight trajectory in cluster k. When $V = 0$, $P(V)|_{V=0}$ in (7) represents the power consumption of the UAV for hovering as

$$P_{hov} = P(V)|_{V=0} = P_0 + P_i, \tag{9}$$

where P_{hov} is a constant. Then the total energy consumption

of hovering in cluster k is expressed as

$$E_k^{hov} = \sum_{m=1}^{M_k} P_{hov} t_m^{hov} = \sum_{m=1}^{M_k} (P_0 + P_i)(t_m^e + t_m^t), \quad (10)$$

where $t_m^e + t_m^t$ represents the hovering duration of the UAV on island m. During the energy transfer stage with duration t_m^e, the UAV charges the SNs on island m with power p_m^e. Then the energy consumption of charging the SNs in cluster k, denoted by E_k^{ch}, is given by

$$E_k^{ch} = \sum_{m=1}^{M_k} p_m^e t_m^e. \quad (11)$$

After the UAV receives the data from the SNs in cluster k and returns to the HAP, the HAP charges the UAV with power p_{power}^k for duration t_h, which depends on the total energy consumption of the UAV in (8)-(11), and p_{power}^k satisfies

$$\eta p_{\text{power}}^k |g|^2 t_h \geqslant C_{\max} - C_k(\zeta), \quad (12)$$

where $C_k(\zeta)$ denotes the residual energy of the UAV after the UAV's ζth traversal of the islands in cluster k. (12) indicates that, for the UAV, the amount of the charged energy should be no smaller than the energy consumption of the UAV for traversing the islands in cluster k.

C. Proposed HTN Protocol

During the data transmission stage, the SNs on island m transmit the generated data to the UAV. In order to maintain the freshness of data, if the residual energy of every SN on island m satisfies the corresponding energy constraint so that the UAV could successfully and simultaneously decode all the data from the SNs, SNs use the NOMA protocol for data transmission. Otherwise, SNs adopt the TDMA protocol for data transmission. We name it as the HTN protocol, which unifies the advantages of the TDMA and NOMA protocols. To be specific, at the beginning of the data transmission stage, the SNs on island m transmit the information about their residual energy to the UAV. Then the UAV compares the residual energy of $S_{i,m}$ with the corresponding energy threshold $E_{i,m}^{th}$ for $i \in \{1, 2, \ldots, N_m\}$. If every SN on island m satisfies the energy constraint, i.e., the residual energy of $S_{i,m}$ is no smaller than $E_{i,m}^{th}$, the UAV broadcasts the information about the transmit power $p_{i,m}^N$ of $S_{i,m}$ for the SNs on island m so that SNs adopt the NOMA protocol for data transmission. Otherwise, the UAV broadcasts the information about the transmit power $p_{i,m}^T$ of $S_{i,m}$ for the SNs on island m so that SNs adopt the TDMA protocol for data transmission. In practice, for the UAV, the energy consumption of circuitry and signal processing is much smaller than the energy consumption of flying, hovering, and charging SNs [31]. Accordingly, for TDMA or NOMA, the energy consumption of circuitry and signal processing is usually negligible. Hence it is reasonable to neglect the energy consumption of the UAV resulting from the protocol switching between TDMA and NOMA.

1) TDMA Protocol: If at least one SN on island m does not satisfy the energy constraint, the SNs on island m adopt the TDMA protocol for data transmission. Under the TDMA protocol, every SN on island m transmits data to the UAV with duration t_m^T. $S_{i,m}$ transmits data to the UAV with power $p_{i,m}^T$, and the data rate $R_{i,m}^T$ is expressed as

$$R_{i,m}^T = W \log_2 \left(1 + \frac{p_{i,m}^T |g_{i,m}|^2}{\sigma^2}\right), \quad (13)$$

where W denotes the bandwidth, and σ^2 denotes the noise power at the UAV. Without loss of generality, we use D to represent the minimum amount of data required to be successfully transmitted by every SN. Then the data rate $R_{i,m}^T$ of $S_{i,m}$ needs to satisfy

$$t_m^T R_{i,m}^T \geq D. \quad (14)$$

Under the TDMA protocol, the energy consumption of $S_{i,m}$ can be expressed as

$$E_{i,m}^T = p_{i,m}^T t_m^T. \quad (15)$$

2) NOMA Protocol: If every SN on island m satisfies the energy constraint, the SNs on island m adopt the NOMA protocol for data transmission with duration t_m^N. Under the NOMA protocol, SNs transmit data to the UAV simultaneously, and the UAV eliminates multiuser interference by using successive interference cancellation (SIC) technique [32]. Without loss of generality, we consider channel gains $|g_{1,m}|^2 > |g_{2,m}|^2 > \ldots > |g_{N_m,m}|^2$ hold. As the SN with the worst channel quality harvests the least amount of energy, the descending order of the signal strength received by the UAV from the SNs is the same as that of the channel gains between the UAV and SNs. The UAV with the SIC decoder first decodes the signal from $S_{1,m}$ by treating the other signals as interference. After the signal from $S_{1,m}$ is decoded successfully, it is subtracted from the overlapping signals. Then the signals from $S_{2,m}, S_{3,m}, \ldots, S_{N_m,m}$ are decoded in order by the UAV similarly [33]. Accordingly, when $S_{i,m}$ transmits data with transmit power $p_{i,m}^N$, the data rate $R_{i,m}^N$ is

$$R_{i,m}^N = W \log_2 \left(1 + \frac{p_{i,m}^N |g_{i,m}|^2}{\sum_{j=i+1}^{N_m} p_{j,m}^N |g_{j,m}|^2 + \sigma^2}\right). \quad (16)$$

To ensure that the minimum amount of data D is successfully transmitted by each SN, the data rate $R_{i,m}^N$ of $S_{i,m}$ satisfies

$$t_m^N R_{i,m}^N \geq D. \quad (17)$$

Under the NOMA protocol, the energy consumption of $S_{i,m}$ can be expressed as

$$E_{i,m}^N = p_{i,m}^N t_m^N. \quad (18)$$

Besides, $E_{i,m}^N$ could be adopted as the corresponding energy threshold $E_{i,m}^{th}$ by the UAV for the comparison between the residual energy of $S_{i,m}$ and the energy threshold $E_{i,m}^{th}$.

To integrate the two protocols, we use a binary variable $q_m(\zeta) \in \{0, 1\}$ to represent the adopted transmission protocol by the SNs on island m for the UAV's ζth traversal to V_m. $q_m(\zeta) = 1$ represents that the NOMA protocol is adopted, and $q_m(\zeta) = 0$ represents that the TDMA protocol is adopted. We have $q_m(\zeta)$ as

$$q_m(\zeta) = \prod_{i=1}^{N_m} \lambda_{i,m}(\zeta). \quad (19)$$

According to the energy threshold $E_{i,m}^{th}$ and the residual energy of $S_{i,m}$, the binary variable $\lambda_{i,m}(\zeta)$ in (19) is

$$\lambda_{i,m}(\zeta) = \begin{cases} 1, & E_{i,m}^{th} \leq E_{i,m}(\zeta - 1) + E_{i,m}^h, \\ 0, & \text{otherwise.} \end{cases} \quad (20)$$

Let $t_m^t(\zeta)$ represent the total transmission duration of N_m SNs on island m for the UAV's ζth traversal to V_m. Then we have

$$t_m^t(\zeta) = q_m(\zeta)t_m^N + (1 - q_m(\zeta))N_m t_m^T. \tag{21}$$

Remark: There are many works on HTN protocols [34]–[36]. The main idea of the existing HTN protocols is that the SNs are divided into several groups such that different groups of SNs transmit data at different times using TDMA, while the SNs in the same group transmit data simultaneously using NOMA. The existing HTN protocols are not suitable for this paper from two perspectives. First, NOMA protocol imposes an energy constraint on each SN on the island, which requires long duration of the energy transfer stage, thus the average AoI would be large. Second, adopting the existing HTN protocols means that SNs on each island first need to transmit data simultaneously to a designated SN using NOMA, and then the designated SNs on different islands transmit data to the UAV at different times using TDMA. Due to the two-hop transmission from SNs to the UAV, the average AoI would also be large.

D. AoI Model

The AoI of the data received from the SN can be seen as the amount of time elapsed from the instant when the data is generated to the instant when the UAV offloads the received data to the HAP [19]. To model AoI at time t, we use $u_{i,m}(t)$ to denote the generation time of the most recently received data at the HAP from $S_{i,m}$. The AoI of the data received from $S_{i,m}$ by the HAP at time t, denoted by $a_{i,m}(t)$, is

$$a_{i,m}(t) = t - u_{i,m}(t). \tag{22}$$

Fig. 2 illustrates the AoI of the data received from $S_{i,m}$ at the HAP. In Fig. 2, the time average of age process in the time interval $(0, \tau)$ at the HAP can be calculated as

$$A_{i,m} = \frac{\int_0^\tau a_{i,m}(t)\, dt}{\tau}. \tag{23}$$

Then we have the long-term average AoI of the data from $S_{i,m}$, denoted by $\Delta_{i,m}$, as

$$\Delta_{i,m} = \lim_{\tau\to\infty} A_{i,m}. \tag{24}$$

It is worth noting that there are N_m SNs on island m, M_k islands in cluster k, and K clusters in the UAV-assisted WPCN. Then the long-term average AoI of the data received from all the SNs is

$$\begin{aligned}\bar{\Delta} =& \frac{1}{N}\sum_{m=1}^{M}\sum_{i=1}^{N_m}\Delta_{i,m} \\ =& \frac{1}{N}\sum_{k=1}^{K}\sum_{m=1}^{M_k} N_m \left(\lim_{\xi\to\infty}\frac{\sum_{\zeta=1}^{\xi} Q_{m_k}^{\zeta}}{\sum_{\zeta=1}^{\xi} X_{m_k}(\zeta)}\right),\end{aligned} \tag{25}$$

where $Q_{m_k}^{\zeta}$ is a trapezoidal area for analyzing the AoI of the received data from S_{i,m_k} on the mth island in cluster k (also abbreviated as the m_kth island) for the UAV's ζth traversal to V_{m_k} in the graphical method. $X_{m_k}(\zeta)$ denotes the duration between the timestamp of the finished energy transfer stage on the m_kth island for the UAV's $(\zeta-1)$th traversal to V_{m_k} and that of the finished energy transfer stage on the m_kth island for the UAV's ζth traversal to V_{m_k}.

To facilitate the reading, we summarize the key notations adopted throughout the paper in TABLE II.

TABLE II: Key Notations

Symbol	Definition
N	The number of SNs in the WPCN.
M	The number of islands in the WPCN.
K	The number of clusters in the WPCN.
N_m	The number of SNs on island m.
M_k	The number of islands in cluster k.
$C_{\max}$	Battery capacity of the UAV.
t_m^e	Duration of the UAV charging the SNs on island m.
t_m^t	Duration of the UAV receiving data from SNs on island m.
$S_{i,m}$	The ith SN on island m.
$p_{i,m}^T$	Transmit power of $S_{i,m}$ under the TDMA protocol.
$p_{i,m}^N$	Transmit power of $S_{i,m}$ under the NOMA protocol.
t_m^T	Transmission duration of each SN on island m under the TDMA protocol.
t_m^N	Transmission duration of the SNs on island m under the NOMA protocol.

III. Problem Formulation

In this section, we first obtain the expressions of $Q_{m_k}^{\zeta}$ and $X_{m_k}(\zeta)$ in (25), and then formulate the long-term average AoI-minimal problem.

As shown in Fig. 2, we take the data from S_{i,m_k} as an example to analyze the AoI. The trapezoidal area $Q_{m_k}^{\zeta}$ depends on $X_{m_k}(\zeta)$ and $T_{m_k}(\zeta)$, which represents the duration between the timestamp of the finished energy transfer stage on the m_kth island and that of the data reception by the HAP for the UAV's ζth traversal to V_{m_k}. To obtain the expressions of $X_{m_k}(\zeta)$ and $T_{m_k}(\zeta)$, we divide the duration of $X_{m_k}(\zeta)$ into five phases. Due to the page limit, the analysis of five phases is presented on page 6 of Technical Report [37]. Here we provide the expressions directly, which can be followed intuitively. Regardless of the flight cycle ζ, we note that X_{m_k} represents the duration between two consecutive finished energy transfer stage of the UAV on the m_kth island. Then we have

$$X_{m_k} = K\left(t_d + t_h\right) + \sum_{k=1}^{K}\left(t_{0,k}^f + \sum_{j=1}^{M_k}\left(t_j^{hov} + t_j^f\right)\right), \tag{26}$$

where $t_{0,k}^f$ denotes the duration of the UAV to fly from the HAP to V_{1_k} in cluster k, $t_j^f (1 \le j < M_k - 1)$ denotes the duration for the UAV to fly from V_j to V_{j+1} in the same cluster, and $t_{M_k}^f$ denotes the duration for the UAV to fly from $V_{(M_k)_k}$ in cluster k to the HAP. In (26), $\sum_{k=1}^{K}\left(t_{0,k}^f + \sum_{j=1}^{M_k} t_j^f\right)$ represents the total flying duration of the UAV for one flight cycle, and $K\left(t_d + t_h\right) + \sum_{k=1}^{K}\sum_{j=1}^{M_k} t_j^{hov}$ represents the total hovering duration of the UAV for one flight cycle. Based on the definition of $T_{m_k}(\zeta)$, $T_{m_k}(\zeta)$ is given by

$$T_{m_k} = \sum_{i=m_k}^{M_k}\left(t_i^{hov} + t_i^f\right) - t_{m_k}^e + t_d. \tag{27}$$

According to the definition of average AoI in (25), $Q_{m_k}^{\zeta}$ is the area of an isosceles trapezoid in the jagged area in Fig. 2. Then we rewrite the average AoI as

$$\bar{\Delta} = \frac{1}{2N}\sum_{k=1}^{K}\sum_{m=1}^{M_k} N_m \left(\lim_{\xi\to\infty}\frac{\sum_{\zeta=1}^{\xi} X_{m_k}^2(\zeta) + 2X_{m_k}(\zeta)T_{m_k}(\zeta)}{\sum_{\zeta=1}^{\xi} X_{m_k}(\zeta)}\right), \tag{28}$$

where $X_{m_k}(\zeta)$ and $T_{m_k}(\zeta)$ are given in (26) and (27), respectively.

In the following, we analyze the factors impacting the average AoI of the WPCN. As shown in Fig. 2, for a given SN, the

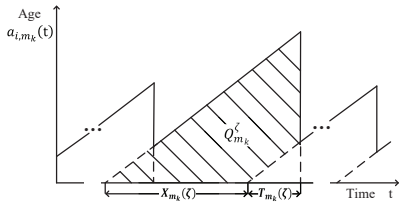

Fig. 2: Age process of the data from S_{i,m_k} on m_kth island.

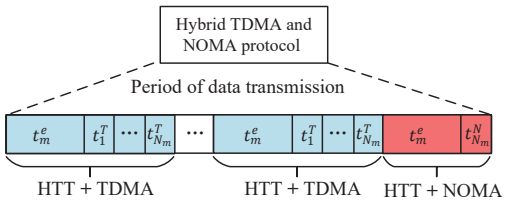

Fig. 3: HTN protocol adopted by the SNs on island m for multiple cycles of the UAV.

average AoI of the data from S_{i,m_k} is determined by the total hovering and flying duration of the UAV traversing the islands. Once the UAV finishes receiving the data from all the SNs in one cluster, it offloads the data to HAP immediately and is fully charged again. Hence for different clusters, the hovering and flying duration of the UAV is independent. In other words, once clustering is completed, the ways of the UAV receiving data from SNs in different clusters are independent. Then, the total hovering and flying duration of the UAV traversing islands in the WPCN is jointly determined by the clustering result such as the number of clusters, and the hovering and flying duration of the UAV traversing every cluster. As the hovering duration on each island is independent and depends on the adopted transmission protocol, i.e., the TDMA protocol or the NOMA protocol, minimizing the hovering duration on every island is equivalent to minimizing the hovering duration in every cluster. The total flying duration depends on the clustering result and the flight trajectory in every cluster. It is worth noting that, different from the case of Fig. 2 focusing on the data received from one SN, the average AoI of data received from all the SNs depends on not only the total hovering and flying duration of the UAV traversing the islands, but also the amount of data received from each island, which is reflected by the number of SNs on each island, i.e., N_m in (28). The reason is that the data from one island is received together, and for the same hovering and flying duration in one cluster, it is straightforward to know that the average AoI for UAV traversing the islands with more SNs early is larger than that for UAV traversing the islands with more SNs later. Fortunately, the flying trajectory design for clusters can take the number of SNs on each island into account.

Therefore, to minimize $\overline{\Delta}$ in (28), we focus on the optimization of the hovering duration of the UAV on island m, determined by the TDMA protocol with power $p_{i,m}^T$ and the NOMA protocol with power $p_{i,m}^N$, the clustering of islands, reflected by K here, and the flight trajectory in every cluster, represented by the traversal sequence of the hovering points in every cluster. Let $\boldsymbol{Q_k} = \{V_{1_k}, V_{2_k}, ..., V_{(M_k)_k}\}$ denote a flight trajectory composed of the hovering points in cluster k. The AoI-minimal problem is formulated as

$$\mathbf{P1}: \min_{(p_{i,m}^T, p_{i,m}^N, \boldsymbol{Q_k})} \bar{\Delta} \tag{29}$$

$$s.t. \quad p_{i,m}^T \geq 0, p_{i,m}^N \geq 0, \tag{29a}$$

$$t_{m_k}^f = \frac{L_{m_k,m_k+1}}{V}, m_k = 0, 1, \ldots, M_k, \tag{29b}$$

$$\sum_{k=1}^{K} \rho_{m,k} = 1, \rho_{m,k} \in \{0,1\}, k = 1, 2, \ldots, K, \tag{29c}$$

$$(6), (12), (14), (17), (19), (20), (21). \tag{29d}$$

Constraint (29b) implies that the flying duration of the UAV is determined by the distance between the consecutive traversed islands, and L_{m_k,m_k+1} represents the distance between the m_kth island and the (m_k+1)th island in cluster k. $L_{0,1}$ represents the distance between the HAP and the 1_kth island in cluster k, and L_{M_k,M_k+1} represents the distance between the $(M_k)_k$th island and the HAP. $\rho_{m,k}$ = 1 indicates that island m belongs to cluster k. Constraint (29c) implies that every island belongs to only one cluster.

IV. Problem Solution

In this section, we first introduce the solution framework, where the average AoI-minimal problem is decomposed into a power allocation subproblem for SNs and a joint clustering of islands and flight trajectory of UAV design subproblem. Then we solve the two subproblems in Section IV-B and Section IV-C, respectively.

A. Solution Framework

Due to the discrete and continuous optimization variables, the average AoI-minimal problem in (29) is non-convex and there are no standard methods to solve it optimally in general. To solve it, we decompose problem P1 into two subproblems: ***the power allocation subproblem for SNs***, called the first subproblem, and ***the joint clustering of islands and UAV's flight trajectory design subproblem***, called the second subproblem. The reasonability of the problem decomposition lies in that the clustering of islands and the UAV's flight trajectory in every cluster are tightly coupled and difficult to be solved separately due to the energy of the UAV, while the two subproblems could be tackled separately by making an approximation. Specifically, the first subproblem aims to minimize the hovering duration of the UAV by optimizing the transmit power of SNs that adopt the proposed HTN protocol in Fig. 3. Apparently, for SNs on each island, the duration of the data transmission stage for SNs using the NOMA protocol is smaller than that using the TDMA protocol. Accordingly, the energy consumption of UAV for hovering under the TDMA protocol is larger. As the unique relation between the two subproblems is the energy of the UAV, we tackle the two subproblems separately by considering the second subproblem is solved under the premise that SNs adopt the TDMA protocol to transmit data. With this approximation, the energy constraint of the UAV could be guaranteed.

1) The First Subproblem Formulation: Under the HTN protocol, the duration of the energy transfer stage and that of the data transmission stage depends on the SN with the worst channel quality on the island, and this duration on

different islands is independent of each other. Then, the power allocation subproblem is formulated as **SP1**.

$$\mathbf{SP1}: \min_{(p_{i,m}^T, p_{i,m}^N)} \lim_{\xi\to\infty} \frac{1}{\xi}\sum_{\zeta=1}^{\xi}\left(t_m^e(\zeta)+t_m^t(\zeta)\right) \tag{30}$$

$$s.t.\ \ p_{i,m}^T \geq 0, p_{i,m}^N \geq 0, i=1,2,\ldots,N_m, \tag{30a}$$

$$t_m^N W\log_2\left(1+\frac{p_{i,m}^N\left|g_{i,m}\right|^2}{\sigma^2+\sum_{j=i+1}^{N_m} p_{j,m}^N\left|g_{j,m}\right|^2}\right)\geq D, \tag{30b}$$

$$t_m^T W\log_2\left(1+\frac{p_{i,m}^T\left|g_{i,m}\right|^2}{\sigma^2}\right)\geq D, \tag{30c}$$

$$t_m^t(\zeta)=q_m(\zeta)t_m^N+(1-q_m(\zeta))N_m t_m^T, \tag{30d}$$

$$\lambda_{i,m}(\zeta)=\begin{cases}1, & E_{i,m}^{th}\leq E_{i,m}(\zeta-1)+E_{i,m}^h,\\ 0, & \text{otherwise},\end{cases} \tag{30e}$$

$$q_m(\zeta)=\prod_{i=1}^{N_m}\lambda_{i,m}(\zeta), m=1,2,\ldots,M_k. \tag{30f}$$

Constraint (30d) represents the duration of the data transmission stage $t_m^t(\zeta)$ for the UAV's ζth traversal to U_m. Constraint (30e) implies that SNs select the TDMA protocol or the NOMA protocol for data transmission based on the corresponding energy threshold.

2) The Second Subproblem Formulation: As aforementioned, the unique relation between the two subproblems is the energy of the UAV. As long as the energy of the UAV could support traversing the cluster, the flight trajectory design in one cluster can be considered as independent of subproblem SP1, while the clustering of islands is tightly coupled with the flight trajectory. To deal with subproblem SP1 and subproblem SP2 independently, we add constraint (31e), where E_k^{hov} is set to be maximum, i.e., the SNs always adopt the TDMA protocol to transmit data. The reason is that compared with the NOMA protocol, the hovering duration with the TDMA protocol is larger, resulting in higher energy consumption of hovering. The joint clustering of islands and UAV's flight trajectory design subproblem is formulated as

$$\mathbf{SP2}: \min_{\boldsymbol{Q_k}} \bar{\Delta} \tag{31}$$

$$s.t.\quad t_{m_k}^f=\frac{L_{m_k,m_k+1}}{V}, m=0,1,\ldots,M_k, \tag{31a}$$

$$\sum_{k=1}^{K} M_k = M, \tag{31b}$$

$$\sum_{k=1}^{K}\rho_{m,k}=1, \rho_{m,k}\in\{0,1\}, k=1,2,\ldots,K, \tag{31c}$$

$$\eta p_{\text{power}}^k\left|g\right|^2 t_h \geqslant C_{\max}-C_k(\zeta), \tag{31d}$$

$$E_k^{hov}+E_k^f+E_k^{ch}\leqslant C_{\max}. \tag{31e}$$

Constraint (31d) implies that the UAV is fully charged by the HAP. Constraint (31e) implies that the UAV has enough energy to traverse every island in the cluster.

B. Solution to SP1: Hovering Duration Optimization

According to the proposed HTN protocol in Section II-C, the UAV needs to ensure that the SN with the worst channel quality has harvested enough energy to transmit data D to the UAV, which has a great impact on the hovering duration of the UAV. Thus, inequalities (30b) and (30c) can be rewritten as equations. The UAV transmits the RF signal to the SNs on island m with duration t_m^e as

$$t_m^e=\frac{p_{N_m,m}t_{N_m}}{\eta p_m^e\left|g_{N_m,m}\right|^2}. \tag{32}$$

The data transmission duration of the SN with the worst channel quality $S_{N_m,m}$ is

$$t_{N_m}=\frac{D}{W\log_2\left(1+\frac{p_{N_m,m}\left|g_{N_m,m}\right|^2}{\sigma^2}\right)}. \tag{33}$$

The parameter $p_{N_m,m}$ in (32) and (33) is replaced by $p_{N_m,m}^T$ for TDMA protocol and $p_{N_m,m}^N$ for NOMA protocol.

1) TDMA Protocol: If the TDMA protocol is adopted by SNs on island m, subproblem SP1 is simplified to minimize

$$\begin{aligned}t_m^e+N_m t_{N_m}&=\frac{p_{N_m,m}^T t_{N_m}}{\eta p_m^e\left|g_{N_m,m}\right|^2}+N_m t_{N_m}\\ &=\frac{D}{W\log_2\left(1+\frac{p_{N_m,m}^T\left|g_{N_m,m}\right|^2}{\sigma^2}\right)}\left(\frac{p_{N_m,m}^T}{\eta p_m^e\left|g_{N_m,m}\right|^2}+N_m\right)\\ &=\frac{D(p_{N_m,m}^T+\eta N_m p_m^e\left|g_{N_m,m}\right|^2)}{\eta p_m^e\left|g_{N_m,m}\right|^2 W\log_2\left(1+\frac{p_{N_m,m}^T\left|g_{N_m,m}\right|^2}{\sigma^2}\right)}.\end{aligned} \tag{34}$$

For convenience of expression, we define $h(p_{N_m,m}^T)=\frac{A(p_{N_m,m}^T+B)}{\log_2\left(1+Cp_{N_m,m}^T\right)}$, where $A=\frac{D}{\eta p_m^e\left|g_{N_m,m}\right|^2 W}$, $B=\eta N_m p_m^e\left|g_{N_m,m}\right|^2$, and $C=\frac{\left|g_{N_m,m}\right|^2}{\sigma^2}$. The first-order derivative of $h(p_{N_m,m}^T)$ with respect to $p_{N_m,m}^T$ is

$$\frac{\mathrm{d}h(p_{N_m,m}^T)}{\mathrm{d}p_{N_m,m}^T}=\frac{A\log_2(1+Cp_{N_m,m}^T)-\frac{AC(p_{N_m,m}^T+B)}{\ln 2(1+Cp_{N_m,m}^T)}}{\log_2(1+Cp_{N_m,m}^T)}. \tag{35}$$

We then define

$$f(p_{N_m,m}^T)=A\log_2(1+Cp_{N_m,m}^T)-\frac{AC(p_{N_m,m}^T+B)}{\ln 2(1+Cp_{N_m,m}^T)}. \tag{36}$$

The first-order derivative of $f(p_{N_m,m}^T)$ with $p_{N_m,m}^T$ is

$$\frac{\mathrm{d}f(p_{N_m,m}^T)}{\mathrm{d}p_{N_m,m}^T}=\frac{AC^2(B+p_{N_m,m}^T)}{\ln 2(1+Cp_{N_m,m}^T)^2}. \tag{37}$$

Since $A>0$, $B>0$, and $C>0$, $\frac{\mathrm{d}f(p_{N_m,m}^T)}{\mathrm{d}p_{N_m,m}^T}$ in (37) is positive. Then $f(p_{N_m,m}^T)$ in (36) increases monotonically with $p_{N_m,m}^T$. We notice that $f(p_{N_m,m}^T)|_{p_{N_m,m}^T\to 0}\to -\frac{ABC}{\ln 2}<0$ and $f(p_{N_m,m}^T)|_{p_{N_m,m}^T\to+\infty}\to+\infty>0$. Thus, there exists a unique $p_{N_m,m}^{T*}$ satisfying $f(p_{N_m,m}^T)=0$, i.e., $\frac{\mathrm{d}h(p_{N_m,m}^{T*})}{\mathrm{d}p_{N_m,m}^{T*}}=0$. Since $\log_2(1+Cp_{N_m,m}^T)>0$, $\frac{\mathrm{d}h(p_{N_m,m}^T)}{\mathrm{d}p_{N_m,m}^T}<0$ for $(0,p_{N_m,m}^{T*})$ and $\frac{\mathrm{d}h(p_{N_m,m}^T)}{\mathrm{d}p_{N_m,m}^T}>0$ for $(p_{N_m,m}^{T*},+\infty)$. That is to say, $h(p_{N_m,m}^T)$ decreases with $p_{N_m,m}^T$ for $p_{N_m,m}^T\in(0,p_{N_m,m}^{T*})$, and increases with $p_{N_m,m}^T$ for $p_{N_m,m}^T\in(p_{N_m,m}^{T*},+\infty)$. Therefore, the minimum $h(p_{N_m,m}^T)$ is achieved at $p_{N_m,m}^{T*}$. Then, the optimal duration of the energy transfer stage on island m, denoted by t_m^{e*}, can be expressed as

$$t_m^{e*}=\frac{p_{N_m,m}^{T*}t_{N_m}^*}{\eta p_m^e\left|g_{N_m,m}\right|^2}, \tag{38}$$

and the optimal duration of the UAV for receiving data from $S_{N_m,m}$, denoted by $t^*_{N_m}$, can be expressed as

$$t^*_{N_m} = \frac{D}{W \log_2\left(1 + \frac{p^{T*}_{N_m,m}|g_{N_m,m}|^2}{\sigma^2}\right)}. \quad (39)$$

2) NOMA Protocol: If the NOMA protocol is adopted by SNs, subproblem SP1 in (30) could be simplified to minimize $t^e_m + t_{N_m}$ by optimizing the transmit power of the SNs on island m. As every SN needs to meet the minimum amount of data D, i.e., $t_{N_m} R^N_{i-1,m} = t_{N_m} R^N_{i,m} = D$, the $S_{i,m}$ and $S_{i-1,m}$ with adjacent received power levels at the UAV satisfies

$$\frac{p^N_{i,m}|g_{i,m}|^2}{\sum_{j=i+1}^{N_m} p^N_{j,m}|g^m_{j,m}|^2 + \sigma^2} = \frac{p^N_{i-1,m}|g^m_{i-1,m}|^2}{\sum_{j=i}^{N_m} p^N_{j,m}|g^m_{j,m}|^2 + \sigma^2}. \quad (40)$$

Based on (40), we have

$$Z_{i-1,m} = \frac{Z^2_{i,m}}{\sum_{j=i+1}^{N_m} Z_{j,m} + \sigma^2} + Z_{i,m}, \quad (41)$$

where $Z_{i,m} = p^N_{i,m}|g_{i,m}|^2$. Since the transmit power of $S_{N_m,m}$ is determined, we obtain the transmit power of SNs on island m according to (41).

C. Solution to SP2: Joint Clustering of Islands and UAV's Flight Trajectory Optimization

The tight coupling between the clustering of islands and UAV's flight trajectory makes subproblem SP2 much more complicated and complex. To tackle it, we propose the clustering-based dynamic adjustment of the shortest path (C-DASP) algorithm composed of three sub-algorithms, i.e., merging-aided K-means clustering (MaKMC) algorithm, particle swarm optimization (PSO) algorithm, and dynamic adjustment (DA) algorithm. The reason why we use three sub-algorithms to tackle subproblem SP2 is that, as we discussed in Section III, two factors, i.e., the flying duration and the amount of data from each island which is reflected by the number of SNs on each island, should be taken into account in the design of AoI-oriented UAV's flight trajectory. Hence two sub-algorithms are needed to address the issue of the UAV's flight trajectory. Specifically, the proposed MaKMC algorithm, which combines the classic K-means clustering (KMC) algorithm and the added merging operation of clusters, tackles the issue of the clustering of islands. The key difference between the MaKMC and KMC algorithms lies in the merging operation of clusters. Actually, the KMC algorithm is used to provide an initial clustering of islands. The reason why we use the KMC algorithm is that the KMC algorithm is always implemented as a standard clustering method in lot of researches [38] due to its advantages of simplicity, efficiency, and stable performance [27]. To fully utilize the energy in the UAV's battery, i.e., reduce the number of times that the UAV is charged by the HAP, the merging operation is performed to merge several small clusters into a new cluster, which is in accordance with the real demand. The PSO and proposed DA algorithms are jointly used to tackle the issue of the UAV's flight trajectory, i.e., the traversal sequence of the hovering points by the UAV. Thereinto, the PSO algorithm is to find the shortest path in every cluster so as to minimize the UAV's flying duration. Based on the traversal sequence of the hovering points obtained by the PSO algorithm, the DA algorithm is utilized to obtain UAV's final flight trajectory by taking into account the number of SNs on each island. The reason why we employ PSO algorithm to find the shortest path in every cluster is that compared with other heuristic algorithms, such as differential evolution, genetic algorithm, and fireworks algorithm, PSO algorithm has fewer parameters and enjoys faster convergence [39].

Algorithm 1 C-DASP algorithm.

Input: The geographical locations of the hovering points on M islands, i.e., $\{x_1, x_2, \ldots, x_M\}$, the number of SNs on M islands, i.e., $\{N_1, N_2, \ldots, N_M\}$, the battery capacity of the UAV $C_{\max}$;
Output: The traversal sequence of the hovering points, denoted by $\boldsymbol{Q}$;

1: Adopt Algorithm 2 to divide islands into K clusters;
2: **for** $k = 1$ to K **do**
3: Select cluster k, adopt Algorithm 3 and Algorithm 4 to obtain the traversal sequence of the hovering points in cluster k;
4: Calculate the total energy consumption of the UAV for traversing the hovering points in cluster k;
5: **while** The total energy consumption of the UAV in cluster k or any cluster that is divided from cluster k is larger than $C_{\max}$ **do**
6: Adopt Algorithm 2 to further divide the islands in the cluster;
7: **for** Each cluster that is divided from cluster k **do**
8: Select the cluster according to the index of the new clustering results of the islands in order;
9: Adopt Algorithm 3 and Algorithm 4 to obtain the traversal sequence of the hovering points in the selected cluster;
10: Calculate the total energy consumption of the UAV in the cluster;
11: **end for**
12: **end while**
13: **end for**
14: **for** each cluster **do**
15: Select the corresponding adjacent cluster to merge into a new cluster;
16: Adopt Algorithm 3 and Algorithm 4 to obtain the traversal sequence of the hovering points in new cluster;
17: Calculate the total energy consumption of the UAV for traversing the hovering points in new cluster;
18: **if** The total energy consumption of the UAV in the merged cluster is larger than $C_{\max}$ **then**
19: The merging operation of clusters is invalidated.
20: **end if**
21: **end for**
22: **return** $\boldsymbol{Q}$.

To clearly state the proposed C-DASP algorithm, we present it in Algorithm 1. In line 1, we adopt Algorithm 2, i.e., the KMC algorithm, to divide the islands according to the locations of the hovering points on islands. After that, we need to ensure that for each cluster, the UAV has enough energy to hover over the islands to complete the tasks of energy transfer and data reception, and fly according to the traversal sequence of the hovering points determined by the PSO and DA algorithms. Hence, in lines 3 and 4, we adopt Algorithm 3, i.e., the PSO algorithm, and Algorithm 4, i.e., the DA algorithm, to obtain the traversal sequence of the hovering points in cluster k, and derive the energy consumption of the UAV traversing cluster k. In lines 5-12, when the energy consumption of the

Algorithm 2 KMC algorithm.

Input: The geographical locations of the hovering points on M islands, i.e., $\{x_1, x_2, \ldots, x_M\}$;
Output: The clusters $\{C_i | i = 1, \ldots, K\}$, the geographical locations of cluster centroids Y;
1: Initialize K;
2: Randomly initialize the geographical locations of K cluster centroids $Y = \{y_1, y_2, \ldots, y_K\}$;
3: **repeat**
4: **for** $i = 1$ to M **do**
5: **for** $j = 1$ to K **do**
6: Calculate the distance between island x_i and cluster centroid y_j;
7: **end for**
8: Update the clusters according to the nearest cluster centroid of the island;
9: **end for**
10: **for** $i = 1$ to K **do**
11: Calculate the location of the new cluster centroid $\mathbf{y}_i$ according to (42);
12: **end for**
13: **until** Y remains unchanged;
14: **return** C_i and Y.

UAV traversing cluster k exceeds battery capacity $C_{\max}$, we further divide the islands in the current cluster k according to the geographical locations of the hovering points on islands. This process continues until all the islands are divided and the UAV has enough energy to fly and hover in every cluster.

In lines 14-21, the merging operation is performed to merge two geographically close clusters into a new cluster, as long as the UAV has enough energy to traverse the new cluster. Specifically, as we adopt the KMC algorithm to divide the islands into K clusters in lines 1-12, the UAV may have residual energy after traversing all the hovering points for some clusters. In order to fully utilize the energy in the UAV's battery, two adjacent clusters are merged into a new cluster according to the geographical locations of the cluster centroids. The merging operation also decreases the unnecessary distance of the flight trajectory, especially the distance between the HAP and the first visited island and the distance between the last visited island and the HAP for each cluster. If two clusters are merged, we adopt the PSO and DA algorithms to obtain the traversal sequence of the hovering points in new cluster, and calculate the total energy consumption of the UAV for traversing the new cluster. Only if the calculated energy consumption of the UAV is no more than its battery capacity $C_{\max}$, the merging operation is valid; Otherwise, it is invalidated. The process of merging operation continues until all clusters can no longer be merged, and we obtain the traversal sequence of the hovering points by the UAV in each cluster. It is worth noting that the proposed MaKMC combines the KMC algorithm and merging operation, while the PSO and DA algorithms are invoked between the KMC algorithm and merging operation. This means that the MaKMC is permeated into the C-DASP algorithm and cannot be presented separately.

In the following, we respectively provide the KMC, PSO and DA algorithms that are incorporated by the proposed C-DASP algorithm in Algorithm 1.

1) KMC Algorithm: As shown in Algorithm 2, we divide M islands into K clusters, i.e., $\{C_i | i = 1, \ldots, K\}$, and the set of the hovering points in cluster i is represented by $C_i = \{x_1, \ldots, x_{M_i}\}$. In line 1, we initialize the number of clusters K. In line 2, the geographical locations of K cluster centroids are randomly initialized. In lines 4-9, update the clusters according to the nearest cluster centroid of the islands from the hovering points. In lines 10-12, the geographical locations of cluster centroids are updated as

$$y_i = \frac{\sum_{x \in C_i} x}{|C_i|}, \tag{42}$$

where $|C_i|$ represents the number of the hovering points in cluster i, and y_i represents the average geographical location of the hovering points in cluster i. The loop in Algorithm 2 stops until the hovering points of the islands in the clusters do not change.

***Lemma* 1.** In the UAV-assisted WPCN with the same number of SNs on each island, we divide islands into K clusters according to the geographical locations of the hovering points on islands. When the UAV traverses the hovering points in each cluster by the shortest path algorithm, the optimal average AoI is achieved.

Proof: As aforementioned in Section III, the average AoI of data received from all the SNs is determined by the hovering duration, the clustering of islands, and the flight trajectory. The hovering duration has been minimized by the proposed HTN protocol in Section IV-B, and the clustering of islands has been given by the KMC algorithm. Then the unique factor impacting the average AoI is the flight trajectory of the UAV. As we discussed in Section III, in the flight trajectory design, we should take both the flying duration of the UAV and the number of SNs on each island into account. Here, the number of SNs on each island is the same, i.e., N_m is the same for all m in (28). In other words, the number of SNs does not affect the flight trajectory, and the optimal flight trajectory design is equivalent to achieve the minimum flying duration in each cluster. Therefore, the optimal average AoI would be achieved when the UAV traverses the hovering points according to the shortest path in each cluster. ■

As is well known, traveling salesman problem (TSP) is an NP-hard problem [40] that aims to find the shortest path to visit each city and return to the departure city. Inspired by TSP, we map each island in one cluster into a city. Similarly, the flight trajectory design problem for the clustering of islands in subproblem SP2 can be proved as the NP-hard problem. According to Lemma 1, we next adopt the PSO algorithm to find the shortest path among a given set of islands with the same number of SNs.

2) PSO Algorithm: The PSO algorithm, consisting of particles for searching the flight trajectory of the UAV, is a heuristic searching approach to find the global optimal traversal sequence by moving the virtually deployed particles [41]. The optimal traversal sequence, obtained from the last iteration $iter$ that particle i believes, is viewed as the individual optimal traversal sequence $\boldsymbol{p}_i^{iter}$. The optimal traversal sequence, obtained from the last iteration $iter$ that the particles believe, is viewed as the global optimal traversal sequence

Algorithm 3 PSO algorithm.

Input: The number of islands M_k in cluster k, the number of particles N_p, the number of iterations N_{iter}, the parameters of PSO algorithm $\{\omega_{\max}, \omega_{\min}, c_1, c_2\}$;
Output: The optimal traversal sequence of the hovering points in cluster k, denoted by $\boldsymbol{Q_k^0} = \{V_{1_k}, V_{2_k}, \ldots, V_{(M_k)_k}\}$;
Initialize the traversal sequence of the hovering points by particle i, denoted by $\boldsymbol{x}_i^0 = \{V_{1_k}^i, V_{2_k}^i, \ldots, V_{(M_k)_k}^i\}$;
Calculate the distance of the flight trajectory of particle i, denoted by $\hat{p}(i)$;
for $iter = 1$ to N_{iter} **do**
  Update inertia coefficient ω according to (43);
  Update $\mathbb{P}_{iter}$ and $\mathbb{G}_{iter}$ according to (46) and (47);
  for $i = 1$ to N_p **do**
    for $j = 1$ to M_k **do**
      Update $\boldsymbol{\vartheta}_i^{iter}$ according to (45);
    end for
  end for
  for $i = 1$ to N_p **do**
    Update $\boldsymbol{g}_i^{iter}$, and $\boldsymbol{p}_i^{iter}$;
  end for
end for
Take the global optimal traversal sequence as the optimal traversal sequence $\boldsymbol{Q_k^0}$.
return $\boldsymbol{Q_k^0}$.

$\boldsymbol{g}_i^{iter}$. In iteration $iter+1$, particle i traverses the hovering points according to $\boldsymbol{p}_i^{iter}$ or $\boldsymbol{g}_i^{iter}$ in (44)-(47). The iteration process stops until the number of iterations N_{iter} is reached. As in Algorithm 3, the PSO algorithm is specified as follows.

Step 1: Initializing the traversal sequence of the hovering points by particle i in cluster k, denoted by $\boldsymbol{x}_i^0 = \{V_{1_k}^i, V_{2_k}^i, \ldots, V_{(M_k)_k}^i\}$.

Step 2: According to $\boldsymbol{x}_i^0$, we calculate the distance of the flight trajectory of particle i as fitness, denoted by $\hat{p}(i)$, and the global optimal fitness is also initialized as $\hat{g}(0)$.

Step 3: Updating inertia coefficient ω as

$$\omega = \omega_{\max} - \frac{(\omega_{\max} - \omega_{\min}) * iter}{N_{iter}}, \tag{43}$$

where $\omega_{\max}$ represents the maximum inertia coefficient, and $\omega_{\min}$ represents the minimum inertia coefficient.

Step 4: According to $\boldsymbol{p}_i^{iter}$ and $\boldsymbol{g}_i^{iter}$, we update the flying velocity of particle i, denoted by $\boldsymbol{\vartheta}_i^{iter+1}$, during the iteration $iter+1$. The rule of updating $\boldsymbol{\vartheta}_i^{iter+1}$ is

$$\begin{aligned}\boldsymbol{\vartheta}_i^{iter+1} &= \omega\boldsymbol{\vartheta}_i^{iter} + c_1\left(\boldsymbol{p}_i^{iter} - \boldsymbol{x}_i^{iter}\right) + c_2\left(\boldsymbol{g}_i^{iter} - \boldsymbol{x}_i^{iter}\right)\\ &= \omega\boldsymbol{\vartheta}_i^{iter} + c_1\boldsymbol{d}_i^{iter} + c_2\boldsymbol{D}_i^{iter},\end{aligned} \tag{44}$$

where c_1 represents the cognition coefficient, and c_2 represents the social coefficient [41]. The flying velocity of particle i satisfies

$$\vartheta_i^{iter}(j) = \begin{cases} d_i^{iter}(j), & d_i^{iter}(j) \neq 0,\\ D_i^{iter}(j), & D_i^{iter}(j) \neq 0,\\ 0, & w < R_0, \end{cases} \tag{45}$$

where R_0 is a random number in $[0,1]$. $\mathbb{P}_{iter}$ is a $N_p \times M_k$ matrix consisting of $\boldsymbol{d}_i^{iter}$, and $d_i^{iter}(j)$ in (45) satisfies

$$d_i^{iter}(j) = \begin{cases} p_i^{iter}(j) - x_i^{iter}(j), & c_1 \geqslant R_1,\\ 0, & c_1 < R_1, \end{cases} \tag{46}$$

where R_1 is a random number in $[0,1]$. $\mathbb{G}_{iter}$ is a $N_p \times M_k$ matrix consisting of $\boldsymbol{D}_i^{iter}$, and $D_i^{iter}(j)$ in (45) satisfies

$$D_i^{iter}(j) = \begin{cases} g_i^{iter}(j) - x_i^{iter}(j), & c_2 \geqslant R_2,\\ 0, & c_2 < R_2, \end{cases} \tag{47}$$

where R_2 is a random number in $[0,1]$.

Step 5: Updating the individual optimal traversal sequence $\boldsymbol{p}_i^{iter}$ by particle i according to $\boldsymbol{\vartheta}_i^{iter}$ in (44);

Step 6: During iteration $iter$, we select the traversal sequence with the minimum fitness as the global optimal traversal sequence, denoted by $\boldsymbol{g}_i^{iter}$ for particle i, and the minimum fitness is denoted by $\hat{g}(iter)$.

Step 7: If the number of iterations is reached, i.e., $iter = N_{iter}$, the loop stops. Then we take the global optimal traversal sequence as the optimal traversal sequence $\boldsymbol{Q_k^0}$. Otherwise, we update $iter = iter + 1$, and go to Step 3.

In the UAV-assisted WPCN where the number of SNs on each island is different, the optimal traversal sequence of the hovering points is not the shortest path in the cluster. In order to find the optimal traversal sequence of the hovering points by the UAV in one cluster, we further propose a DA algorithm to dynamically adjust the traversal sequence of the hovering points obtained by PSO algorithm to reduce the average AoI.

3) DA Algorithm: According to the PSO algorithm, we have obtained the traversal sequence of the hovering points with the shortest distance by the UAV in every cluster. However, the amount of data received from SNs on each island also has an important impact on the average AoI. To obtain better AoI performance, the UAV is willing to fly later to the island that has more amount of data. The amount of data depends on the number of SNs on each island. To capture the effect of the number of SNs on each island on the average AoI, we propose the DA algorithm for dynamic adjustment of the traversed hovering points in Algorithm 4. The traversal sequence obtained by the PSO algorithm is adopted as the initial traversal sequence. The rules for dynamic adjustment of the traversed hovering points are specified as follows. If the number of SNs on the island that currently needs to be adjusted is larger than the number of SNs on the island that is traversed by the UAV after this adjusted island in the traversal sequence, we swap the sequence of the two hovering points and recal-

Algorithm 4 DA algorithm.

Input: The traversal sequence determined by the PSO algorithm in cluster k, denoted by $\boldsymbol{Q_k^0} = \{V_{1_k}, V_{2_k}, \ldots, V_{(M_k)_k}\}$, the number of SNs on islands in cluster k, denoted by $\boldsymbol{N_s} = \{N_{1,k}, N_{2,k}, \ldots, N_{M_k,k}\}$;
Output: The traversal sequence of the hovering points in cluster k, denoted by $\boldsymbol{Q_k} = \{V_{1_k}^{'}, V_{2_k}^{'}, \ldots, V_{(M_k)_k}^{'}\}$;
for $i = 1$ to $M_k - 1$ **do**
  for $j = i+1$ to M_k **do**
    if $N_{i,k} \geqslant N_{j,k}$ **then**
      Swap V_{i_k} and V_{j_k} in the traversal sequence.
    end if
    Calculate the AoI under the updated traversal sequence.
    If the obtained AoI is less than that obtained under the previous traversal sequence, update the traversal sequence as $\boldsymbol{Q_k}$.
  end for
end for
return $\boldsymbol{Q_k}$.

culate the average AoI obtained by the UAV according to the current swaped traversal sequence. If the obtained average AoI is smaller, the adjusted traversal sequence is updated as the traversal sequence for comparison. When the average AoI does not change, the dynamic adjustment rules stop.

V. Simulation Results and Discussions

In this section, we evaluate the average AoI performance of the UAV-assisted WPCN under the proposed HTN protocol and the C-DASP algorithm. The UAV-assisted WPCN consists of one HAP, one UAV, 40 islands. The number of SNs on each island is randomly generated, and the total number of SNs is 593. The flight height h and the speed of the UAV V are set as 10 m and 20 m/s, respectively. The battery capacity $C_{\max}$ of the UAV is 28 kJ. The parameters about the rotary-wing UAV's flight power are listed as follows [29]. The tip speed of the rotor blade U_{tip} is set as 120 m/s. The mean rotor induced velocity when hovering v_0 is set as 4.03. The fuselage drag ratio d_0 and rotor solidity s are set as 0.6 and 0.05, respectively. The air density ρ and rotor disc area A are set as 1.225 kg/m^3 and 0.503 m^2, respectively. The UAV transmits the RF signal to the SNs on island m with transmit power $P_m^e = 1$ W. The islands are randomly distributed in a square area with side length of 1000 m. The HAP is located at the center of this square area, i.e., $(500, 500, 0)$. N_m SNs are randomly distributed on island m with the radius of 50 m, where $N_m \geq 1$ is a random number. The topology is not limited to the scenario of island environmental monitoring, and is generally suitable for the scenarios where nodes are clustered around certain fixed hotpots, like Fig. 5 in [42], or monitoring areas are scattered, like Fig. 8 in [9] and Fig. 7 in [42]. The system bandwidth is set as $W = 4$ MHz [20], the energy conversion efficiency is set as $\eta = 0.8$, and the path-loss factor is set as $\alpha = 2$. The gain of the channel at the reference distance 1 m is set as $\kappa = -50$ dB, and the noise power $\sigma^2 = -100$ dBm [20]. The data size is set as $D = 1$ Mb [19]. Besides, the parameters of the PSO algorithm are set as $\omega_{\max} = 0.85$, $\omega_{\min} = 0.5$, $N_p = 500$, and $N_{iter} = 1000$. All the parameters are set as described above unless otherwise specified.

A. Verification of the proposed HTN Protocol

Fig. 4 displays the average AoI versus the number of SNs on one island for HTN, TDMA, and NOMA protocols when the number of UAV's flight cycle equals 100. It is easy to observe that the average AoI under three protocols increases with the number of SNs on one island. The reason is that the increasing number of SNs on one island would lead to the increasing duration of data transmission stage for TDMA protocol and that of energy transfer stage for NOMA protocol. Besides, we observe that when the number of SNs on one island is small, the average AoI under the NOMA protocol is smaller than that under the TDMA protocol, and vice versa. This is due to the reason that for the small number of SNs, i.e., 2, 3 in Fig. 4, the energy thresholds of supporting the NOMA protocol are relatively low and could be satisfied quickly by SNs. However, with the continuously increasing number of

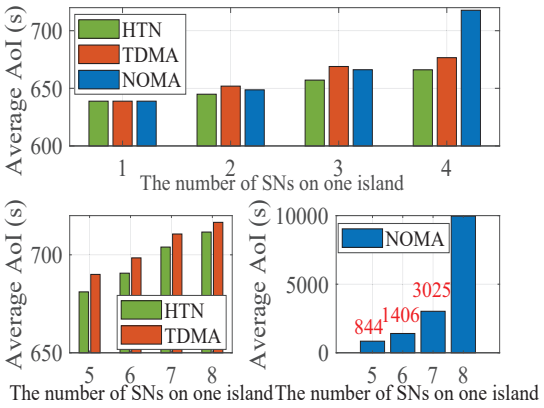

Fig. 4: The average AoI versus the number of SNs on one island for HTN, TDMA and NOMA protocols.

SNs on one island, i.e., 4, 5, ..., 8 in Fig. 4, the SNs need to harvest more energy to reach the corresponding energy thresholds of supporting the NOMA protocol according to (41), and then the duration of energy transfer stage would become longer. This observation gives us a different direction to design another HTN protocol, i.e., the NOMA protocol is applied on the islands with small number of SNs, while the TDMA protocol is applied on the islands with large number of SNs. Another important observation is that, the average AoI under the HTN protocol is always the smallest among the three transmission protocols. The reason is that, compared with the TDMA protocol, the HTN protocol shortens the duration of data transmission stage for the UAV. Compared with the NOMA protocol, the HTN protocol shortens the duration of energy transfer stage for SNs.

B. AoI Performance Analysis and Verification of the Proposed C-DASP Algorithm

Fig. 5 plots the clusterings and flight trajectories of the UAV under KMC and MaKMC algorithms for different network topologies, i.e., topology 1 in Figs. 5(a)-(b) and topology 2 in Figs. 5(c)-(d). For topology 1 with 218 SNs distributed in the area of 1000∗1000, compared with the clustering results in Fig. 5(a), we observe that clusters 4 and 5 are merged in a new cluster in Fig. 5(b). As a result, the average AoI decreases from 690s to 664s. The reason is that the energy of the fully-charged UAV should have supported the UAV traversing two clusters in Fig. 5(a), which causes the UAV frequently returns to the HAP and increases the total flying duration. We provide a different network topology, i.e., topology 2 with 241 SNs distributed in the area of 1200∗1200, to show the generality of the MaKMC algorithm. By comparing Fig. 5(c) with Fig. 5(d), we also observe that clusters 1 and 5 in Fig. 5(c) are merged into a new cluster in Fig. 5(d), and accordingly, the average AoI decreases from 779s to 749s. It is worth noting that the merging operation aims to make full use of the energy in the UAV's battery, i.e., reduce the number of times that the UAV is charged by the HAP, which is in accordance with the real demand. Meanwhile, it is also an attempt to reduce the average AoI, and as shown in Fig. 5, the merging operation is beneficial for the average AoI in some cases of the UAV-

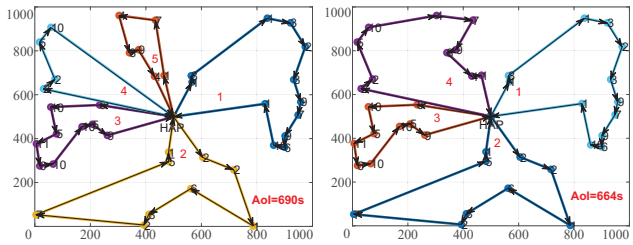

(a) Topology 1 under KMC (b) Topology 1 under MaKMC

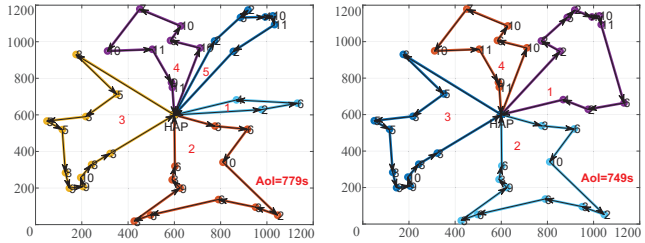

(c) Topology 2 under KMC (d) Topology 2 under MaKMC

Fig. 5: Clusterings and flight trajectories under KMC and MaKMC algorithms for different network topologies.

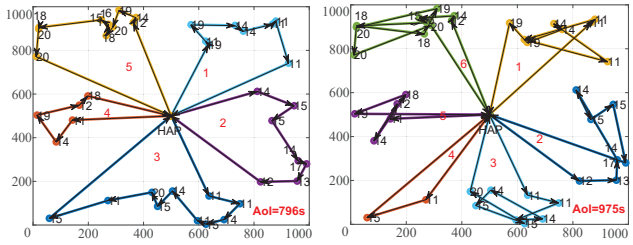

(a) C-SP (b) C-WS

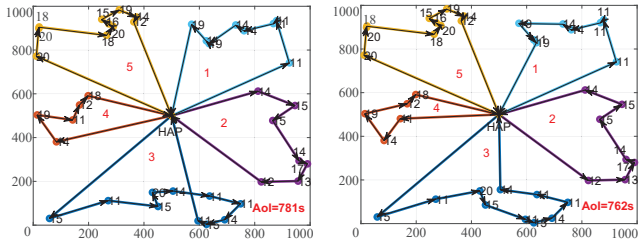

(c) C-WPS (d) C-DASP

Fig. 6: Clusterings and flight trajectories under the proposed C-DASP and other comparison algorithms.

assisted WPCN. In other words, the merging operation fully utilizes the energy in the UAV's battery but may not always be beneficial for the average AoI.

Fig. 6 shows the clusterings and flight trajectories of the UAV under the proposed C-DASP and other three algorithms. The algorithms for comparison, i.e., the clustering-based shortest path (C-SP) algorithm, the clustering-based weighted scheduling (C-WS) algorithm, the clustering-based weighted path scheduling (C-WPS) algorithm, are specified as follows.

- C-SP algorithm: In every cluster, the traversal sequence of the hovering points is obtained by the shortest path algorithm [9], [43], such as the PSO algorithm.
- C-WS algorithm: In every cluster, the traversal sequence of the hovering points is determined by the ascending order of the number of SNs on islands.
- C-WPS algorithm: This algorithm, proposed by us for comparison, also takes both flight distance/duration and the number of SNs on one island into account. It aims to find the traversal sequence of the hovering points that minimizes the sum of the products for each island, and the product is calculated by the number of SNs on the island and the distance from the current hovering point to the HAP along the traversal sequence.

As shown in Fig. 6, the number of clusters under the C-SP algorithm in Fig. 6(a) is the least with 5, and that under the C-WS algorithm in Fig. 6(b) is the largest with 6. While the number of clusters under the C-WPS algorithm in Fig. 6(c) and the proposed C-DASP algorithm in Fig. 6(d) are in the range $[5, 6]$. The reason is that the flight trajectory determined by the C-SP algorithm is the shortest without considering the impact of the number of SNs on each island on the average AoI. Hence the energy of the fully-charged UAV could support the UAV traversing more islands for once flight, and then the number of clusters in the UAV-assisted WPCN is the least. On the contrary, the flight trajectory determined by the C-WS algorithm is entirely based on the number of SNs on each island without considering the flight distance. Thus, compared with that of the C-SP algorithm, the number of islands traversed by the fully-charged UAV for once flight is less, and then there are more clusters in the UAV-assisted WPCN. While the C-WPS and the proposed C-DASP algorithms jointly consider the impacts of flight distance and the number of SNs on each island on the average AoI, hence the number of islands traversed by the fully-charged UAV for once flight would be not more than that under the C-SP algorithm, and meanwhile not less than that under the C-WS algorithm. As shown in Fig. 6(a), Fig. 6(c), and Fig. 6(d), even the number of clusters under the C-WPS and the proposed C-DASP algorithms are equal to that under the C-SP algorithm, we can also clearly observe that the flight distance in cluster 3 determined by the C-WPS and the proposed C-DASP algorithms is greater than that determined by the C-SP algorithm. Moreover, we observe that although the flight distance in clusters 1 and 2 is the same for Fig. 6(a) and Fig. 6(d), the traversal sequence of the hovering points is completely reciprocal. The same observation could be obtained in cluster 1 for Fig. 6(a) and Fig. 6(c). This is due to the reason that both the C-WPS and the proposed C-DASP algorithms not only consider the flight distance but also the number of SNs on each island. Fig. 6 also shows that for the given topology, the average AoI under the proposed C-DASP algorithm is the smallest among the four algorithms, and a general discussion about the AoI performance will be presented in Fig. 7.

Fig. 7(a) shows the average AoI versus the total number of SNs in the WPCN under four algorithms. When the horizontal coordinate is $[1, 10]$, the number of SNs on each island belongs to $[1, 10]$. When the horizontal coordinate is $[11, 20]$, the number of SNs on each island belongs to $[11, 20]$. The rest can be deduced by analogy. Fig. 7(b) shows the average AoI versus the heterogeneity of the number of SNs on islands under

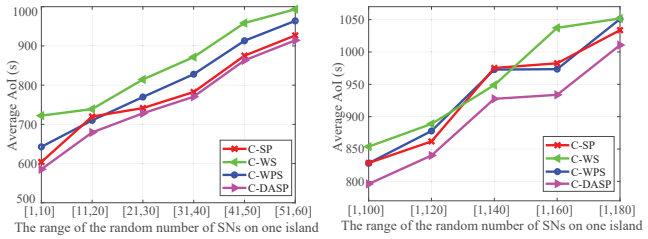

(a) (b)

Fig. 7: (a) The average AoI versus the total number of SNs on in the WPCN. (b) The average AoI versus the heterogeneity of the number of SNs on islands.

four algorithms. The relationship between the average AoI and the total number of SNs in the WPCN can be observed by Fig. 7(a). Thus, for the horizontal coordinate in Fig. 7(b), we not only ensure the increase of the heterogeneity of the number of SNs on islands, but also the increase of the total number of SNs in the WPCN (i.e., control variables). Specifically, when the horizontal coordinate is $[1, 100]$, for 40 islands in the WPCN, the number of SNs on each island belongs to $[1, 100]$. When the horizontal coordinate is $[1, 120]$, for 35 islands, the number of SNs on each island belongs to $[1, 100]$, and for 5 islands, the number of SNs on each island belongs to $(100, 120]$. When the horizontal coordinate is $[1, 140]$, for 30 islands, the number of SNs on each island belongs to $[1, 100]$; for 5 islands, the number of SNs on each island belongs to $(100, 120]$; and for 5 islands, the number of SNs on each island belongs to $(120, 140]$. The rest can be deduced by analogy. By comparing Fig. 7(b) with Fig. 7(a), the impact of the heterogeneity of the number of SNs on islands could be observed.

Then, we present the observations from Fig. 7. (I) We observe from both Fig. 7(a) and Fig. 7(b) that, the proposed C-DASP algorithm always achieves the minimal average AoI, which verifies the superiority of the proposed algorithm. The reason is that compared with the C-SP algorithm, the C-DASP algorithm takes the impact of the number of SNs on each island, i.e., N_m, into account. Compared with the C-WS algorithm, the C-DASP algorithm takes the impact of the flight distance into account. Although the C-WSP algorithm also takes the two impacts into account, Fig. 7 shows that the C-DASP algorithm is more superior than it. (II) We observe from Fig. 7(a) that, with the increase of the number of SNs on each island, the average AoI increases, since the UAV hovers over each island with longer duration for transmitting the RF signal to SNs and receiving data from SNs. Besides, we observe that the average AoI under the C-SP algorithm is always smaller than that under the C-WS algorithm, since the heterogeneity of the number of SNs on islands keeps almost unchanged, and the flight distance has a dominant impact on the flight trajectory design. (III) We observe from Fig. 7(b) that, the average AoI under the C-SP algorithm sometimes is larger than that under the C-WS algorithm, which demonstrates that the heterogeneity of the number of SNs on islands sometimes has a dominant impact on the flight trajectory design.

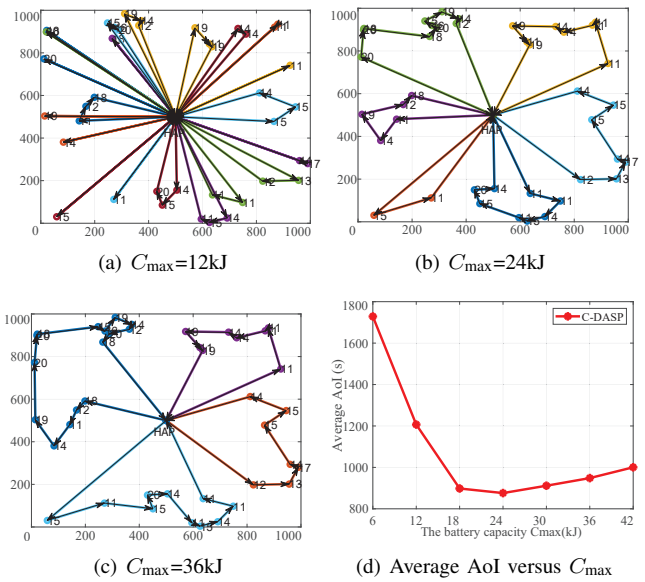

(a) $C_{\max}$=12kJ (b) $C_{\max}$=24kJ

(c) $C_{\max}$=36kJ (d) Average AoI versus $C_{\max}$

Fig. 8: The flight trajectories versus the battery capacity of UAV with (a) 12kJ, (b) 24kJ, and (c) 36kJ. (d) The average AoI versus the battery capacity of UAV.

C. Impacts of Battery Capacity and Flight Height of the UAV

Fig. 8 depicts the impact of the battery capacity of UAV $C_{\max}$ on the flight trajectories and the average AoI. From Figs. 8(a)-(c), we observe that with the increase of $C_{\max}$, the number of clusters in the WPCN decreases. This observation can be attributed to the clustering of islands which is based on the full utilization of the energy in the UAV's battery. From Fig. 8(d), we observe that the average AoI first decreases with $C_{\max}$ and then increases with $C_{\max}$. The reason is that there is a tradeoff between the duration from the timestamp of data generation in a given cluster to that of data offloading and the duration from the timestamp of starting to traverse other clusters to that of the next data generation in the given cluster. This tradeoff can be represented in a more intuitive manner, i.e., the tradeoff between the number of clusters and the total flying and hovering duration in one cluster. It is worth noting that the tradeoff exists since we try to reduce the number of times that the UAV is charged when clustering. We then present the reason in a specific way by combining with Figs. 8(a)-(c). When $C_{\max}$ is small with 12kJ as in Fig. 8(a), the number of clusters in the WPCN is relatively large, the UAV needs to frequently return to the HAP to offload the received data and be fully charged. In this case, although the received data from one cluster is offloaded timely, the time for the UAV frequently returning to the HAP results in the long duration for traversing other clusters, which is the dominant factor impacting the average AoI for the small $C_{\max}$ and decreases with $C_{\max}$. Therefore, with the increase of $C_{\max}$ for $C_{\max} \in$ (6kJ, 24kJ), the average AoI becomes smaller. When $C_{\max}$ is large with 36kJ as in Fig. 8(c), the number of clusters in the WPCN is relatively small, and then the frequency for the UAV returning to the HAP decreases. In this case, although the duration for traversing other clusters is reduced, the long total flying and hovering duration of the

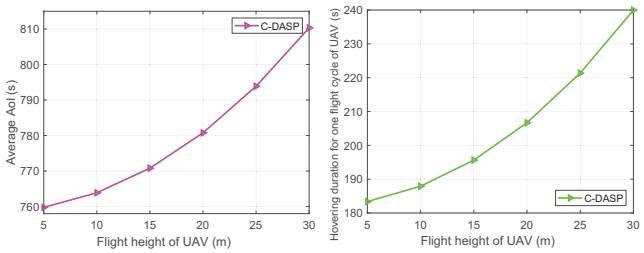

(a) (b)

Fig. 9: (a) The average AoI versus the flight height of the UAV. (b) Hovering duration for one flight cycle of the UAV versus the flight height of the UAV.

UAV in one cluster results in the untimely data offloading, which is the dominant factor impacting the average AoI for the large $C_{\max}$ and becomes more serious with the increase of $C_{\max}$. Therefore, with the increase of $C_{\max}$ for $C_{\max} \in (24\text{kJ}, 42\text{kJ})$, the average AoI becomes larger. These observations provide directions on how to select the battery capacity of the UAV to minimize the average AoI, as well as make full use of the battery energy of the UAV.

Fig. 9 depicts the impact of the flight height of the UAV on the average AoI. We observe from Fig. 9(a) that the average AoI increases with the flight height of the UAV. The reason is that, with the increase of the flight height of the UAV, the channel qualities between the UAV and SNs become worse. As a result, the UAV requires longer time to charge SNs and receive data from SNs. That is to say, the hovering duration of the UAV on each island increases with the flight height of the UAV, as shown in Fig. 9(b).

VI. Conclusion

In a UAV-assisted WPCN for the island environmental monitoring, we analyzed the key factors affecting the long-term average AoI with consideration of the battery recharging of the UAV. Based on the key factors, we formulated the long-term average AoI-minimal problem by jointly optimizing the transmit power of SNs, the clustering of islands, and UAV's flight trajectory. To address the NP-hard problem, we decoupled it into two subproblems: the power allocation subproblem, which was solved by proposing a HTN protocol for SNs, and the joint clustering of islands and UAV's flight trajectory design subproblem, which was solved by proposing a C-DASP algorithm. Simulation results showed that: (1) the HTN protocol achieves smaller AoI than the TDMA protocol and the NOMA protocol; (2) The merging operation for clustering is beneficial for reducing the number of times that the UAV is charged, and the dynamic adjustment operation based on the number of SNs on each island in the C-DASP algorithm contributes to achieve better AoI performance; (3) There is a tradeoff between the number of clusters and the total flying and hovering duration of the UAV in one cluster caused by the battery capacity of the UAV under the C-DASP algorithm. Future works include more practical network models, such as the deployment of multiple UAVs, and more comprehensive approaches, such as the reinforcement learning approach.

References

[1] K. Zheng, R. Luo, X. Liu, J. Qiu, and J. Liu, " Distributed DDPG-based resource allocation for age of information minimization in mobile wireless-powered Internet of Things," *IEEE Internet Things J.*, DOI: 10.1109/JIOT.2024.3406044, 2024.

[2] X. Liu, B. Xu, K. Zheng, and H. Zheng, "Throughput maximization of wireless-powered communication network with mobile access points," *IEEE Trans. Wireless Commun.*, vol. 22, no. 7, pp. 4401-4415, Jul. 2023.

[3] L. Xie, J. Xu, and R. Zhang, "Throughput maximization for UAV-enabled wireless powered communication networks," *IEEE Internet Things J.*, vol. 6, no. 2, pp. 1690-1703, Apr. 2019.

[4] M. Samir, C. Assi, S. Sharafeddine, and A. Ghrayeb, "Online altitude control and scheduling policy for minimizing AoI in UAV-assisted IoT wireless networks," *IEEE Trans. Mob. Comput.*, vol. 21, no. 7, pp. 2493-2505, Jul. 2022.

[5] T. Taleb, A. Ksentini, H. Hellaoui, and O. Bekkouche, "On supporting UAV based services in 5G and beyond mobile systems," *IEEE Netw.*, vol. 35, no. 4, pp. 220-227, Jul. 2021.

[6] L. Xie, X. Cao, J. Xu, and R. Zhang, "UAV-enabled wireless power transfer: A tutorial overview," *IEEE Trans. Green Commun. Netw.*, vol. 5, no. 4, pp. 2042-2064, Dec. 2021.

[7] X. Yuan, T. Yang, Y. Hu, J. Xu, and A. Schmeink, "Trajectory design for UAV-enabled multiuser wireless power transfer with nonlinear energy harvesting," *IEEE Trans. Wireless Commun.*, vol. 20, no. 2, pp. 1105-1121, Feb. 2021.

[8] H. Yan, Y. Chen, and S. -H. Yang, "Time allocation and optimization in UAV-enabled wireless powered communication networks," *IEEE Trans. Green Commun. Netw.*, vol. 6, no. 2, pp. 951-964, Jun. 2022.

[9] H. Pan, Y. Liu, G. Sun, J. Fan, S. Liang, and C. Yuen, "Joint power and 3D trajectory optimization for UAV-enabled wireless powered communication networks with obstacles," *IEEE Trans. Commun.*, vol. 71, no. 4, pp. 2364-2380, Apr. 2023.

[10] Q. Tang, Y. Yang, L. Liu, and K. Yang, "Minimal throughput maximization of UAV-enabled wireless powered communication network in cuboid building perimeter scenario," *IEEE Trans. Netw. Serv. Man.*, vol. 20, no. 4, pp. 4558-4571, Dec. 2023.

[11] K. Liu and J. Zheng, "UAV trajectory optimization for time-constrained data collection in UAV-enabled environmental monitoring systems," *IEEE Internet Things J.*, vol. 9, no. 23, pp. 24300-24314, Dec. 2022.

[12] T. Taleb, N. Sehad, Z. Nadir, and J. Song, "VR-based immersive service management in B5G mobile systems: A UAV command and control use case," *IEEE Internet Things J.*, vol. 10, no. 6, pp. 5349-5363, Mar. 2023.

[13] J. Liu, P. Tong, X. Wang, B. Bai, and H. Dai, "UAV-aided data collection for information freshness in wireless sensor networks," *IEEE Trans. Wireless Commun.*, vol. 20, no. 4, pp. 2368-2382, Apr. 2021.

[14] S. Kaul, R. Yates, and M. Gruteser, "Real-time status: How often should one update," in *Proc. IEEE INFOCOM*, Orlando, FL, USA, Mar. 2012, pp. 2731-2735.

[15] R. D. Yates, Y. Sun, D. R. Brown, S. K. Kaul, E. Modiano, and S. Ulukus, "Age of information: An introduction and survey," *IEEE J. Sel. Areas Commun.*, vol. 39, no. 5, pp. 1183-1210, May 2021.

[16] M. Yi, X. Wang, J. Liu, Y. Zhang, and B. Bai, "Deep reinforcement learning for fresh data collection in UAV-assisted IoT networks," in *Proc. IEEE INFOCOM WKSHPS*, Toronto, ON, Canada, Jul. 2020, pp. 716-721.

[17] M. A. Abd-Elmagid and H. S. Dhillon, "Average peak age-of-information minimization in UAV-assisted IoT networks," *IEEE Trans. Veh. Technol.*, vol. 68, no. 2, pp. 2003-2008, Feb. 2019.

[18] B. Zhu, E. Bedeer, H. Nguyen, R. Barton, and G. Zhen, "UAV trajectory planning for AoI-minimal data collection in UAV-aided IoT networks by transformer," *IEEE Trans. Wireless Commun.*, vol. 22, no. 2, pp. 1343-1358, Feb. 2023.

[19] H. Hu, K. Xiong, G. Qu, Q. Ni, P. Fan, and K. B. Letaief, "AoI-minimal trajectory planning and data collection in UAV-assisted wireless powered IoT networks," *IEEE Internet Things J.*, vol. 8, no. 2, pp. 1211-1223, Jan. 2021.

[20] L. Liu, K. Xiong, J. Cao, Y. Lu, P. Fan, and K. B. Letaief, "Average AoI minimization in UAV-assisted data collection with RF wireless power transfer: A deep reinforcement learning scheme," *IEEE Internet Things J.*, vol. 9, no. 7, pp. 5216-5228, Apr. 2022.

[21] O. Oubbati, M. Atiquzzaman, A. Lakasand, A. Baz, H. Alhakami, and W. Alhakami, "Multi-UAV-enabled AoI-aware WPCN: A multi-agent reinforcement learning strategy," in *Proc IEEE INFOCOM WKSHPS*, Vancouver, BC, Canada, May 2021, pp. 1-6.

[22] O. Oubbati, M. Atiquzzaman, H. Lim, A. Rachedi, and A. Lakas, "Synchronizing UAV teams for timely data collection and energy transfer by deep reinforcement learning," *IEEE Trans. Veh. Technol.*, vol. 71, no. 6, pp. 6682-6697, Jun. 2022.

[23] G. Ahani, D. Yuan, and Y. Zhao, "Age-optimal UAV scheduling for data collection with battery recharging," *IEEE Commun. Lett.*, vol. 25, no. 4, pp. 1254-1258, Apr. 2021.

[24] E. Eldeeb, J. D. S. Santana, D. E. Perez, M. Shehab, N. H. Mahmood, and H. Alves, "Multi-UAV path learning for age and power optimization in IoT with UAV battery recharge," *IEEE Trans. Veh. Technol.*, vol. 72, no. 4, pp. 5356-5360, Apr. 2023.

[25] M. Zeng, N. -P. Nguyen, O. A. Dobre, and H. V. Poor, "Delay minimization for NOMA-assisted MEC under power and energy constraints," *IEEE Wireless Commun. Lett.*, vol. 8, no. 6, pp. 1657-1661, Dec. 2019.

[26] X. Gao, X. Zhu, and L. Zhai, "AoI-sensitive data collection in multi-UAV-assisted wireless sensor networks," *IEEE Trans. Wireless Commun.*, vol. 22, no. 8, pp. 5185-5197, Aug. 2023.

[27] F. Nie, Z. Li, R. Wang, and X. Li, "An effective and efficient algorithm for K-means clustering with new formulation", *IEEE Trans. Knowledge Data Eng.*, vol. 35, no. 4, pp. 3433-3443, Apr. 2023.

[28] H. Yang, Y. Ye, X. Chu, and S. Sun, "Energy efficiency maximization for UAV-enabled hybrid backscatter-harvest-then-transmit communications," *IEEE Trans. Wireless Commun.*, vol. 21, no. 5, pp. 2876-2891, May 2022.

[29] Y. Zeng, J. Xu, and R. Zhang, "Energy minimization for wireless communication with rotary-wing UAV," *IEEE Trans. Wireless Commun.*, vol. 18, no. 4, pp. 2329-2345, Apr. 2019.

[30] X. Liu, X. Li, K. Zheng, and J. Liu, "AoI minimization of ambient backscatter-assisted EH-CRN with cooperative spectrum sensing," *Computer Networks*, vol. 245, Article ID 110389, May 2024.

[31] D. Yang, Q. Wu, Y. Zeng, and R. Zhang, "Energy tradeoff in ground-to-UAV communication via trajectory design," *IEEE Trans. Veh. Technol.*, vol. 67, no. 7, pp. 6721-6726, Jul. 2018.

[32] H. Pan, J. Liang, S. C. Liew, V. C. M. Leung, and J. Li, "Timely information update with nonorthogonal multiple access," *IEEE Trans. Ind. Informat.*, vol. 17, no. 6, pp. 4096-4106, Jun. 2021.

[33] K. Chi, Z. Chen, K. Zheng, Y. Zhu, and J. Liu, "Energy provision minimization in wireless powered communication networks with network throughput demand: TDMA or NOMA?," *IEEE Trans. Commun.*, vol. 67, no. 9, pp. 6401-6414, Sept. 2019.

[34] D. Zhang, Q. Wu, M. Cui, G. Zhang, and D. Niyato, "Throughput maximization for IRS-assisted wireless powered hybrid NOMA and TDMA," *IEEE Wireless Commun. Lett.*, vol. 10, no. 9, pp. 1944-1948, Sept. 2021.

[35] X. Wei, H. Al-Obiedollah, K. Cumanan, W. Wang, Z. Ding, and O. A. Dobre, "Spectral-energy efficiency trade-off based design for hybrid TDMA-NOMA system," *IEEE Trans. Veh. Technol.*, vol. 71, no. 3, pp. 3377-3382, Mar. 2022.

[36] X. Wei, H. Al-Obiedollah, K. Cumanan, Z. Ding, and O. A. Dobre, "Energy efficiency maximization for hybrid TDMA-NOMA system with opportunistic time assignment," *IEEE Trans. Veh. Technol.*, vol. 71, no. 8, pp. 8561-8573, Aug. 2022.

[37] X. Liu, H. Liu, K. Zheng, J. Liu, T. Taleb, and N. Shiratori, "AoI-minimal clustering, transmission and trajectory co-design for UAV-assisted WPCNs," Technical Report from TechRxiv Preprint, https://doi.org/10.36227/techrxiv.24003576, 2023.

[38] Z. Kaleem, W. Khalid, A. Muqaibel, A. A. Nasir, C. Yuen, and G. K. Karagiannidis, "Learning-aided UAV 3D placement and power allocation for sum-capacity enhancement under varying altitudes," *IEEE Commun. Lett.*, vol. 26, no. 7, pp. 1633-1637, Jul. 2022.

[39] J. Zhang, Y. Lu, Y. Wu, C. Wang, D. Zang, A. Abusorrah, and M. Zhou, "PSO-based sparse source location in large-scale environments with a UAV swarm," *IEEE Trans. Intell. Transp. Syst.*, vol. 24, no. 5, pp. 5249-5258, May 2023.

[40] A. Bera, S. Misra, C. Chatterjee, and S. Mao, "CEDAN: Cost-effective data aggregation for UAV-enabled IoT networks," *IEEE Trans. Mob. Comput.*, vol. 22, no. 9, pp. 5053-5063, Sept. 2023.

[41] W. Zhang and W. Zhang, "An efficient UAV localization technique based on particle swarm optimization," *IEEE Trans. Veh. Technol.*, vol. 71, no. 9, pp. 9544-9557, Sept. 2022.

[42] Z. Wei, M. Zhu, N. Zhang, L. Wang, Y. Zou, Z. Meng, H. Wu, and Z. Feng, "UAV-assisted data collection for Internet of Things: A survey," *IEEE Internet Things J.*, vol. 9, no. 17, pp. 15460-15483, Sept. 2022.

[43] G. Chen, C. Cheng, X. Xu, and Y. Zeng, "Minimizing the age of information for data collection by cellular-connected UAV," *IEEE Trans. Veh. Technol.*, vol. 72, no. 7, pp. 9631-9635, Jul. 2023.

Xiaoying Liu (Senior Member, IEEE) received the B.E. degree in Electronic Engineering from Nanjing University of Science and Technology, Nanjing, China, in 2013, and the Ph.D. degree in Electronic Engineering from Shanghai Jiao Tong University, Shanghai, China, in 2018. Currently, she is an associate professor with the School of Computer Science and Technology, Zhejiang University of Technology, Hangzhou, China. Her research interests include AIoT, wireless cooperative networks, and wireless powered communication networks.

Huihui Liu received the M.E. degree in software engineering from Zhejiang University of Technology, Hangzhou, China, in 2024. Her research interests include UAV, age of information and wireless-powered communication networks.

Kechen Zheng (Senior Member, IEEE) received the B. E. degree in Electronic Engineering from Shanghai Jiao Tong University, China, in 2013 and Ph.D. degree in Electronic Engineering in the same university in 2018. He is currently an associate professor with the School of Computer Science and Technology, Zhejiang University of Technology, Hangzhou, China. His research interests include IoT, performance evaluation in cognitive networks, and energy harvesting wireless communication networks.

Jia Liu (Senior Member, IEEE) received the Ph.D. degree from the School of Systems Information Science, Future University Hakodate, Japan, in 2016. His research interests include wireless systems security, space-air-ground integrated networks, Internet of Things, 6G, etc. He received the 2016 and 2020 IEEE Sapporo Section Encouragement Award.

Tarik Taleb (Senior Member, IEEE) received the B.E. degree (with distinction) in information engineering and the M.Sc. and Ph.D. degrees in information sciences from Tohoku University, Sendai, Japan, in 2001, 2003, and 2005, respectively. He is currently a Full Professor at Ruhr University Bochum, Germany. His current research interests include AI-based network management, architectural enhancements to mobile core networks, network softwarization and slicing, mobile cloud networking, network function virtualization, software-defined networking, software-defined security, and mobile multimedia streaming.

Norio Shiratori (Life Fellow, IEEE) received his Ph.D. degree from Tohoku University in 1977. Recognizing his significant contributions, he was honored with the title of IEEE Life Fellow in 2017. Since 2017, he has been serving as a Professor at Research and Development Initiative, Chuo University. Prof. Shiratori has published over 15 books and over 600 refereed papers in computer science and related fields. He is a fellow of the Japan Foundation of Engineering Societies (JFES), the Information Processing Society of Japan (IPSJ), and the Institute of Electronics, Information and Communication Engineers (IEICE). He was a recipient of the Minister of MEXT Award from the Japanese Government in 2016, the Science and Technology Award from the Ministry of Education, Culture, Sports, Science, and Technology (MEXT) in 2009, the IEICE Achievement Award in 2001, the IEICE Contribution Award in 2011, the IPSJ Contribution Award in 2008, and the IEICE Honorary Member in 2012.